Brain, Behavior, & Immunity - Health 42 (2024) 100879

Contents lists available at ScienceDirect

Brain, Behavior, & Immunity - Health

journal homepage: www.editorialmanager.com/bbih/default.aspx

Early-life obesogenic environment integrates immunometabolic and epigenetic signatures governing neuroinflammation

Perla Ontiveros-Ángel [a], Julio David Vega-Torres [a], Timothy B. Simon [a], Vivianna Williams [a], Yaritza Inostroza-Nives [b], Nashareth Alvarado-Crespo [b], Yarimar Vega Gonzalez [b], Marjory Pompolius [c], William Katzka [d], John Lou [e], Fransua Sharafeddin [a], Ike De la Peña [f], Tien Dong [d], Arpana Gupta [d], Chi T. Viet [g], Marcelo Febo [c], Andre Obenaus [h], Aarti Nair [i], Johnny D. Figueroa [a,*]

[a] *Center for Health Disparities and Molecular Medicine and Department of Basic Sciences, Physiology Division, Department of Basic Sciences, Loma Linda University Health School of Medicine, Loma Linda, CA, USA*
[b] *Department of Biochemistry and Pharmacology, San Juan Bautista School of Medicine, Caguas, Puerto Rico, USA*
[c] *Translational Research Imaging Laboratory, Department of Psychiatry, Department of Neuroscience, College of Medicine, University of Florida Health, Gainesville, FL, USA*
[d] *G. Oppenheimer Center for Neurobiology of Stress and Resilience, Vatche and Tamar Manoukian Division of Digestive Diseases, Department of Medicine, David Geffen School of Medicine, UCLA Microbiome Center, University of California, Los Angeles, CA, USA*
[e] *Loma Linda University Health School of Behavioral Health, Loma Linda, CA, USA*
[f] *Department of Pharmaceutical and Administrative Sciences, Loma Linda University Health School of Pharmacy, Loma Linda, CA, USA*
[g] *Department of Oral & Maxillofacial Surgery, Loma Linda University Health School of Dentistry, Loma Linda, CA, USA*
[h] *Department of Pediatrics, University of California Irvine, Irvine, CA, USA*
[i] *Department of Psychology, Loma Linda University, Loma Linda, CA, USA*

ARTICLE INFO

Keywords:
Adolescence
Anxiety
Obesity
Microbiome
Microglia
Neuroinflammation
FKBP5
NODDI

ABSTRACT

Childhood overweight/obesity is associated with stress-related psychopathology, yet the pathways connecting childhood obesity to stress susceptibility are poorly understood. We employed a systems biology approach with 62 adolescent Lewis rats fed a Western-like high-saturated fat diet (WD, 41% kcal from fat) or a control diet (CD, 13% kcal from fat). A subset of rats underwent a 31-day model of predator exposures and social instability (PSS). Effects were assessed using behavioral tests, DTI (diffusion tensor imaging), NODDI (neurite orientation dispersion and density imaging), 16S rRNA gene sequencing for gut microbiome profiling, hippocampal microglia analysis, and targeted gene methylation. Parallel experiments on human microglia cells (HMC3) examined how palmitic acid influences cortisol-related inflammatory responses.

Rats exposed to WD and PSS exhibited deficits in sociability, increased fear/anxiety-like behaviors, food consumption, and body weight. WD/PSS altered hippocampal microstructure (subiculum, CA1, dentate gyrus), and microbiome analysis showed a reduced abundance of members of the phylum *Firmicutes*. WD/PSS synergistically promoted neuroinflammatory changes in hippocampal microglia, linked with microbiome shifts and altered *Fkbp5* expression/methylation. In HMC3, palmitate disrupted cortisol responses, affecting morphology, phagocytic markers, and cytokine release, partially mediated by FKBP5.

This study identifies gene-environment interactions that influence microglia biology and may contribute to the connection between childhood obesity and stress-related psychopathology later in life.

1. Introduction

Childhood obesity is a severe medical problem affecting more than 340 million children and adolescents worldwide (Organization WH, 2016). While obesity is a complex disease, consuming Western-style diets (WD) is a significant factor contributing to the global pediatric obesity epidemic (Moreno et al., 2010). Obesity and consuming imbalanced obesogenic WD, typically rich in saturated fats and simple sugars,

* Corresponding author.
E-mail address: jfigueroa@llu.edu (J.D. Figueroa).

https://doi.org/10.1016/j.bbih.2024.100879
Received 24 September 2024; Accepted 29 September 2024
Available online 2 October 2024

have emerged as risk factors for developing psychiatric disorders (Bornstein et al., 2006; Opel et al., 2020; Salari-Moghaddam et al., 2018; Scott et al., 2008; Simon et al., 2006). The prolonged COVID-19-related lockdowns, social instability, and uncertainty stress negatively impacted dietary practices and increased childhood stress and obesity prevalence rates (Abawi et al., 2020; Lange et al., 2021; Woolford et al., 2021). Exposure to these impinging obesogenic environmental factors during childhood may have profound long-term effects on the brain and shape adult behavior and health. Hence, it is imperative to elucidate the biological pathways and mechanisms that connect early exposure to obesogenic environments with mental health outcomes in later life.

While many complex linkages connect childhood obesity to psychopathology, stress susceptibility is a significant pathway (Bremner et al., 2020). There is extensive literature describing shared pathological pathways in obesity and stress-related psychiatric disorders (Opel et al., 2020; Michopoulos et al., 2016; Milaneschi et al., 2019; Wolf et al., 2017). Obesity influences inflammatory mediators, the sympathetic nervous system, and the hypothalamic-pituitary-adrenal (HPA) axis. Recent investigations highlight the potential involvement of extra-hypothalamic brain areas, such as the hippocampus, in obesity neuropsychiatric comorbidities (Jacka et al., 2015; Cherbuin et al., 2015; Mestre et al., 2017; Raji et al., 2010).

The hippocampus is critical in terminating the physiological stress responses via feedback inhibition of the hypothalamic-pituitary-adrenal (HPA) axis (Jacobson and Sapolsky, 1991; Ulrich-Lai and Herman, 2009). Thus, alterations in this brain region may contribute to the stress-related psychiatric co-morbidities associated with obesity. Reduced hippocampal volume has emerged as a prominent anatomical endophenotype in human obesity (Jacka et al., 2015; Cherbuin et al., 2015; Mestre et al., 2017; Raji et al., 2010). In line with these studies, we reported that access to an obesogenic diet during adolescence 1) reduces the volume of the hippocampus (Kalyan-Masih et al., 2016), 2) impairs the maturation of corticolimbic circuits (Vega-Torres et al., 2018), 3) enhances behavioral vulnerabilities to psychosocial stressors (Kalyan-Masih et al., 2016; Vega-Torres et al., 2018, 2019), and 4) increases oxidative stress and neuroinflammation (Santana et al., 2021), even in the absence of an obesogenic phenotype (Vega-Torres et al., 2022a). However, there is limited understanding of the mechanisms that lead to hippocampal impairments and subsequent susceptibility to stress in individuals exposed to obesogenic environments during adolescence.

Obesity is associated with reduced synaptic density in humans (Asch et al., 2021) and rodents (Cope et al., 2018; Hao et al., 2016). Several genes implicated with human obesity are critical in sustaining synaptic integrity, supporting the evidence for links between synaptic integrity and the disease (Locke et al., 2015). Microglia are the innate immune cells of the brain. These highly dynamic cells play significant roles in axonal remodeling, synaptic pruning(Schafer and Stevens, 2013), and hippocampal tissue volume (Nelson et al., 2021). Microglia are highly responsive to stress (Li et al., 2021; Frank et al., 2019), obesogenic diets (Vega-Torres et al., 2022a; Cope et al., 2018; Hao et al., 2016) and are involved in the behavioral outcomes associated with obesity (Cope et al., 2018; Sobesky et al., 2014; Guillemot-Legris and Muccioli, 2017). However, the underlying molecular mechanisms regulating microglia activities in obesogenic environments remain poorly understood.

Microglia respond to local signals within the brain and receive input from the periphery, including dietary lipids, cytokines, hormones, and other immune modulators. Obesogenic dietary factors like palmitate and glucocorticoid stress hormones control microglia morphology and functions (Butler et al., 2020; Drew and Chavis, 2000; Tracy et al., 2013; Wang et al., 2012a; Xu et al., 2019). In addition, preclinical findings suggest that the gut microbiome plays a pivotal role in regulating microglial maturation and function (Cryan and Dinan, 2015; Erny and Prinz, 2020; Mosher and Wyss-Coray, 2015), which can impact brain maturation (Paolicelli et al., 2011; Rea et al., 2016). Because both obesity and stress are also associated with lasting epigenetic changes, a possible hypothesis is that access to an obesogenic diet during the critical maturational period of adolescence could confer stress susceptibility later in life through epigenetic effects on microglial genes involved in immunometabolic function. An essential modulator of these interactions is FKBP5 (Häusl et al., 2019; Criado-Marrero et al., 2020; Balsevich et al., 2014; Schmidt et al., 2015), (Häusl et al., 2019; Criado-Marrero et al., 2020; Balsevich et al., 2014; Schmidt et al., 2015), which codes for the FK506-binding protein 5-51 (FKBP51) and has emerged as a promising drug target for stress-related disorders (Binder et al., 2004, 2008; Yehuda et al., 2016). New studies demonstrate a robust association between the FKBP5/FKBP51 and microglia activities (Gan et al., 2022) and overall hippocampal structure and function (Córdova-Palomera et al., 2017; Fani et al., 2013; Zobel et al., 2010). Thus, FKBP5/FKBP51 may play a role in predisposing obese individuals to stress by regulating microglia and the structural integrity of the hippocampus.

This study investigated the impact of obesogenic environments on adolescent brain maturation. The obesogenic conditions altered neuroimaging metrics in the hippocampus. Our two-hit model of dietary obesity and psychosocial stress proved an excellent method to identify the lasting consequences of these environmental factors on sociability, anxiety-like behavior, startle responses, and fear learning. Diet and stress influenced *FKBP5* expression and methylation states in the hippocampus. *In vitro* studies demonstrated that palmitate primes microglia and altered pro-inflammatory responses to cortisol. Our findings indicate that exposure to an obesogenic diet during the critical maturational period of adolescence leads to unique brain changes that may participate in maladaptive stress reactivity later in life. This comprehensive study holds significant translational and clinical implications, as uncovering risk factor mechanisms for maladaptive stress responses has the potential to profoundly influence both obesity and mental health care.

2. Methods

2.1. Animals

Experimental procedures involving animals complied with protocol No. 20–171 (now 23–0126), approved by the Institutional Animal Care and Use Committee (IACUC) at the Loma Linda University Health School of Medicine. This protocol follows institutional regulations consistent with the National Institutes of Health Guide for the Care and Use of Laboratory Animals and the ARRIVE guidelines for reporting animal research (Sert et al., 2020). Great efforts were made to reduce the animal number and minimize animal suffering and discomfort. Female Lewis dams with 8 male pups (postnatal day 15, PND15) were obtained from Charles River Laboratories (Portage, MI, USA). Upon arrival, female rats were housed with their pups with *ad libitum* access to food and water. The rats were kept in standard housing conditions (12-h light/dark cycle with lights on at 7:00 a.m., 21 ± 2 °C, and relative humidity of 45%). Adolescent male pups (PND21) were weaned, matched across diet groups based on their body weight and startle responses, and paired housed with *ad libitum* access to their assigned diet and water for the duration of the study. The body weights were recorded weekly, and food consumption was quantified at least twice weekly.

The food consumed was measured at the same time of the day (0900–1100 h). Uneaten food (cage top and spillage) was weighted and recorded, and fresh food was added to the top of the cage. Food intake was expressed as kilocalories (kcal) per day.

2.2. Study design

Sixty-two (62) adolescent Lewis rats (PND21) were weaned, carefully matched by body weight and acoustic startle reactivity, and randomized to receive either a Western-like high-saturated fat diet (*WD*, $n = 30$) or an ingredient-matched purified control diet (*CD*, $n = 27$). Five female rats were identified and removed from the study. Any male rat that interacted with a female was also removed from the study. While

acknowledging the limitation posed by utilizing only male rats in this study, the decision to employ male rats exclusively is justified for several reasons. Firstly, focusing exclusively on male rats ensures continuity and consistency in the experimental design and data interpretation, aligning with previous research conducted by our team. Additionally, it simplifies data analysis and interpretation by eliminating potential interactions between sex, development (puberty), and other experimental factors (e.g., diet, stress), thereby enhancing the clarity of the study findings. In summary, the decision to use solely male rats in this initial study on this model is grounded in the principles of continuity, efficiency, and alignment with our established protocols. This approach ensures methodological consistency, reduces the complexity of the study design, and optimizes the scientific rigor and interpretability of the results. It is important to note that our recent studies are expanding to include female rats (Sharafeddin et al., 2024). The final total sample number was 52: CD $n = 24$ and WD $n = 28$, all males. The WD (*Product No. F7462*; Lot No. 248348) is 4.6 kcal/g and 41.4% kcal from fat) and the CD (*Product No. F7463*; Lot No. 248347) 3.7 kcal/g and 12.6% kcal from fat) were obtained from Bio-Serv (Frenchtown, NJ, USA). The macronutrient composition and fatty acid profiles are detailed in previous studies and summarized in Supplementary (S) Table 1 (Vega-Torres et al., 2020, 2022b). The rats consumed the diets for four weeks were further subdivided into four groups using random assignments (at PND49): **(1)** control diet, unexposed (CDU; $n = 13$); **(2)** control diet, exposed (CDE; $n = 14$); **(3)** Western diet, unexposed (WDU; $n = 15$); **(4)** Western diet, exposed (WDE; $n = 15$). Exposed groups underwent a well-established 31-day psychosocial stress (PSS) model, including predator encounters and social instability (Zoladz et al., 2012). At PND82, the effects of WD and PSS were assessed using a comprehensive battery of standard behavioral tests and an array of stress and inflammation markers measures. The day following the completion of behavioral assessments, a randomly selected subset of rats underwent a 12-h fasting period to explore the metabolic effects of the experimental interventions. All the rats were then euthanized, and plasma and brain tissue were collected. Experiments were performed in 4 independent rat sub-cohorts (each with a similar number of animals and containing all study groups). A complete timeline of the study is included in Fig. 1.

2.3. Detailed methods are included in the detailed methods document

2.3.1. Psychosocial stress model (PSS)

This study used a model of psychosocial stress to assess how access to an obesogenic diet impacts the behavioral and physiological outcomes of adolescent trauma. The model involved exposing rats to a natural predator (juvenile cats) and social instability. Predator exposure was achieved by placing the rats in close proximity to soiled cat litter and a freely moving cat in a metal enclosure, conducted twice at a 10-day interval. Social instability was induced by changing the rats' cage partners daily for 31 days, preventing them from being housed with the same partner consecutively. Cage partners were switched daily within the same diet group to minimize cross-contamination risk.

2.3.2. Behavioral test battery

A comprehensive battery of behavioral tests was used to evaluate stress responses in rats consuming an obesogenic diet. The tests included the acoustic startle reflex (ASR), fear-potentiated startle (FPS), elevated plus-maze (EPM), and a modified Y maze to assess social behaviors. Behavioral assessments were conducted between postnatal days (PND) 82–94, primarily during the light phase. The order of tests was arranged

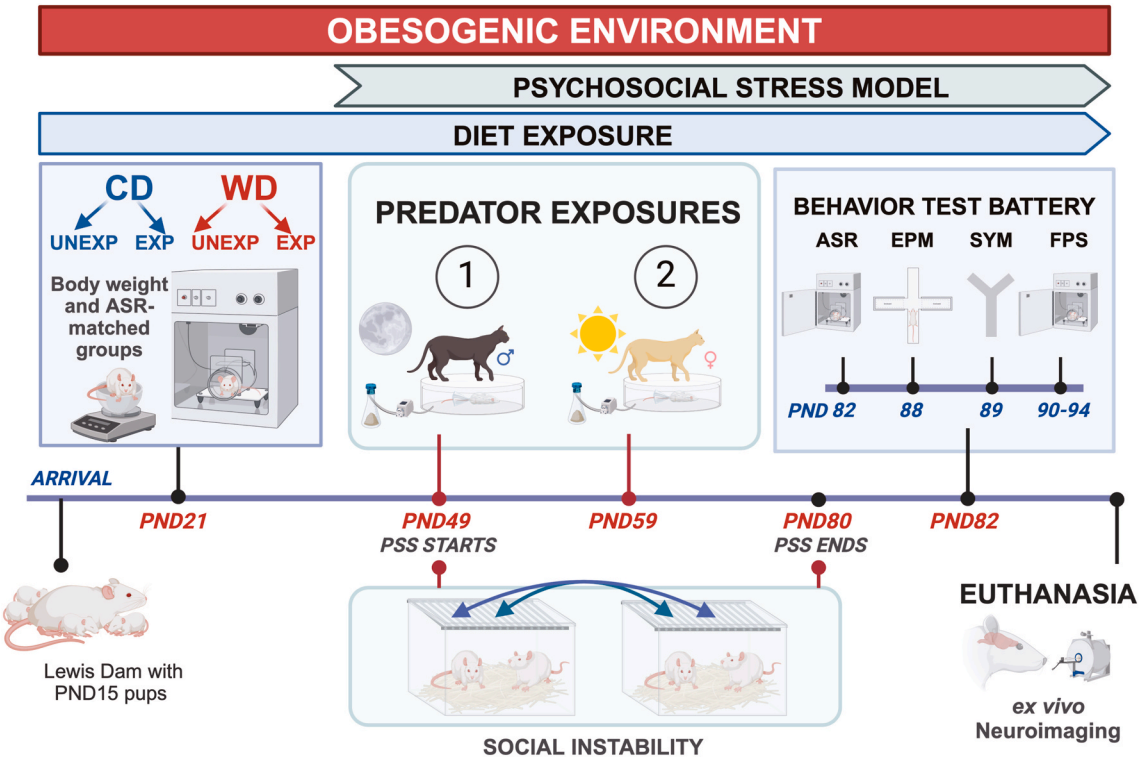

Fig. 1. Experimental timeline and procedures. Adolescent Lewis rats (PND21) were grouped based on body weight and acoustic startle reactivity and assigned to either a Western-like high-saturated fat diet or a purified control diet with matched ingredients. These diets were consumed for four weeks, after which the rats were divided into four groups through random selection at PND49: (1) control diet, unexposed (CDU); (2) control diet, exposed (CDE); (3) Western diet, unexposed (WDU); (4) Western diet, exposed (WDE); each group comprising n = 14 rats. Exposed groups underwent a well-established 31-day psychosocial stress (PSS) model involving predator encounters and social instability. At PND82, the effects of WD and PSS were evaluated using a comprehensive battery of standard behavioral tests and various measures of stress and inflammation markers. Subsequently, all rats were euthanized, and plasma and brain tissue samples were collected. Abbreviations: ASR, Acoustic startle reflex, EPM, Elevated plus maze; SYM, Social Y-Maze; FPS, Fear-potentiated startle.

from least to most invasive to minimize carryover effects.

2.3.3. Acoustic startle reflex (ASR)

The ASR was measured using a startle response system, with rats placed in a nonrestrictive plexiglass stabilimeter within soundproofed chambers. The rats were exposed to acoustic stimuli, and their startle responses were recorded and normalized by body weight. The testing session lasted 22 min, including habituation and presentation of startle-inducing tones.

2.3.4. Fear-potentiated startle (FPS)

FPS was used to assess hippocampal-dependent fear learning by conditioning rats to associate a light stimulus with a footshock. The startle response was measured in the presence and absence of the conditioned stimulus (light) to evaluate fear learning. Fear extinction was tested through subsequent sessions where the rats were exposed to the light without the shock. FPS data were reported as the proportional change in startle response, with increased FPS indicating heightened fear.

2.4. Elevated plus maze (EPM)

The EPM test assessed anxiety-like behaviors by measuring the time rats spent in open arms. Videos were recorded under near-infrared light, were cleaned between trials, and behaviors were tracked using video analysis software. The time spent in open arms indicated anxiety, while the number of closed-arm entries was used to measure locomotor activity.

2.5. Social Y-Maze

Sociability was measured using a modified Y maze where rats were allowed to explore freely, with one arm containing a conspecific and the other containing an inanimate object. The rats' interactions with the conspecific versus the object were recorded and analyzed. The test aimed to assess social preference and was conducted without prior habituation, with results reported as the number of social interactions and the ratio of interactions between the conspecific and the object.

2.6. Tissue collection

Animals were divided into two groups for tissue analysis: neuroimaging and histology (28 rats) and molecular analysis (29 rats). The neuroimaging group was perfused with an isotonic solution followed by paraformaldehyde, with brains fixed and stored in PBS for later processing. The molecular analysis group was perfused with PBS, with brains rapidly dissected and hippocampal tissues preserved in RNAlater™ for RNA stability.

2.7. Metabolic and inflammatory profiling

Corticosterone levels were measured at multiple time points throughout the experimental timeline by extracting and analyzing fecal samples with ELISA. Heart rate and blood pressure were assessed using a tail-cuff plethysmography system, and fasting blood glucose levels were determined from tail blood samples using a glucometer. Inflammatory profiles were analyzed using bead-based immunoassays to quantify various cytokines in plasma samples.

2.8. FKBP5 methylation profiling

Left hippocampal tissue was processed for qRT-PCR and bisulfite sequencing to assess FKBP5 gene methylation. DNA was bisulfite-modified, amplified, and sequenced, with methylation levels calculated based on the ratio of methylated to total reads.

2.9. Microbiome sequencing and analysis

Stool samples were collected, and DNA was extracted for sequencing of the 16S rRNA gene. Sequencing data were processed to determine microbial diversity and composition using DADA2 and QIIME 2, with alpha and beta diversity metrics calculated and differential abundance testing performed using DESeq2.

2.10. Magnetic resonance imaging (MRI)

Rats were anesthetized and perfused with a sucrose and paraformaldehyde solution before brain fixation. Brains were stored in FC-40 for scanning using a high-resolution MRI scanner. Diffusion-weighted imaging was performed, and data were processed to calculate diffusion metrics and analyze brain microstructure using NODDI modeling.

2.11. Neurohistology

Brains were cryoprotected, sectioned, and stained for microglia/macrophage marker Iba-1. Sections underwent visualization.

2.12. Microglial morphological characterization

2.12.1. Image acquisition

Blinded investigators acquired images of Iba-1/DAB-stained tissue sections using a Keyence BZ-9000 microscope at 40 × magnification. A multi-plane virtual-Z mode was used to capture detailed composite images of hippocampal CA1 regions, with at least nine image sets per region per hemisphere, each including at least six Iba-1+ cells, saved in TIFF format.

2.12.2. Image processing and segmentation

Images were processed using ImageJ to create high-quality composites by merging z-stack images. The images were thresholded to enhance contrast, and cells were manually edited to create masks, avoiding bias. The microphotographs were binarized, and filled shape images with masks were saved and analyzed for microglial morphological changes.

2.12.3. Fractal analysis

Fractal analysis was performed with FracLac for ImageJ to quantify microglial morphology using Box Counting (BC) to assess cell complexity. Measurements were averaged from 12 random grid placements, and results were analyzed using GraphPad Prism for statistical significance.

2.12.4. RNAScope

The RNAscope Multiplex Fluorescent v2 Assay was used to visualize mRNA expression for FKBP5 and AIF1. The process involved multiple steps, including fixation, dehydration, and hybridization, followed by signal development and counterstaining with DAPI for microscopy.

2.12.5. Confocal microscopy (RNAScope)

Slides were scanned with a Zeiss LSM 710 NLO confocal microscope to obtain z-stacks of hippocampal CA1 regions.

2.12.6. RNAscope image analysis

IMARIS 10.1 was used to quantify nuclei and puncta of FKBP5 and AIF1, and colocalization was assessed using the "shortest distance" function.

2.13. In vitro assessments

2.13.1. Cell culture

HMC3 cells were cultured in MEM supplemented with FBS and penicillin/streptomycin, and maintained at passages 2 to 10. Before

analysis, cells were serum-starved and then treated with vehicle or palmitic acid for 24 h, followed by an additional incubation with cortisol for 24 h. The treatments included vehicle alone, palmitic acid alone, cortisol alone, or a combination of palmitic acid and cortisol.

2.13.2. Cell viability assay

MTT assays measured cell viability to determine the IC50 of palmitic acid. Cells were treated with varying concentrations of palmitic acid, and absorbance at 570 nm was measured after incubation.

2.13.3. RNA extraction and quantitative real-time PCR

Total RNA was extracted with TRIzol, and cDNA was synthesized. Gene expression for *Fkbp5*, *Il6*, *Tnfa*, and *Nfkb* was quantified using real-time PCR and normalized to *Gapdh* levels.

2.13.4. Gene silencing

Fkbp5 siRNA was transfected into HMC3 cells, followed by hydrocortisone or palmitic acid treatment. RNA was then extracted to assess gene expression changes.

2.13.5. Cytokine quantification

ELISA kits were used to measure IL-6 and TNFα levels in cell culture media from control or treated HMC3 cells.

2.13.6. Confocal microscopy

HMC3 cells were fixed, permeabilized, and stained with CD68 antibody. Cells were then counterstained with DAPI for visualization using confocal microscopy.

2.13.7. Determination of ROS generation

ROS levels were assessed using the Muse Oxidative Stress Kit and dihydroethidium (DHE). The method included validation with NAC and antimycin A to confirm ROS generation.

2.14. Statistical analysis

Data were analyzed using GraphPad Prism, incorporating Shapiro-Wilk and Brown-Forsythe tests to assess distribution and variance. The ROUT method was used to identify outliers, leading to discrepancies between the original and final sample numbers due to removing these outliers. Additionally, five male pups were excluded from the study due to interactions with female rats; these pups were not included in any biological measures. Principal Component Analysis (PCA) and chi-square analyses were performed, along with correlation analyses. Statistical methods included two-way and three-way ANOVAs, Spearman's rank correlations, and post hoc power analysis to evaluate the effects of diet, stress, and other factors on the outcomes. Statistical significance was set at $p < 0.05$.

3. Results

This study investigated brain, behavior, and immunometabolic responses to stress in rats exposed to an obesogenic diet during adolescence. We postulated that intake of an obesogenic Western-like high saturated fat diet (WD) during adolescence would alter responses to chronic psychosocial stress (PSS) (See **Graphical Abstract**). Furthermore, we posited that the WD will impact stress-related anatomical, cellular, and molecular substrates. For enhanced readability, *F* statistics and post hoc test results are fully detailed in Tables 1–8 and S Tables 2–20

Table 2
Statistical Information on microglial morphological measurements in Figs. 3 and 4. Bold denotes significant effects following three-way ANOVA and post hoc comparisons between CD UNEXP, CD EXP, WD UNEXP, and WD EXP. Sample size: Neurohistology: 4 rats/group, Gene Expression: 3 rats/group.

	Iba-1+ cells	Lacunarity	Span Ratio	TNF-α HPC GE
Source of Variation	F Statistic, posthoc	F Statistic, posthoc	F Statistic, posthoc	F Statistic, posthoc
WD x PSS	F(1, 12) = 0.4530, *p* = 0.5137	F(1, 12) = 0.3175, *p* = 0.5835	F(1, 12) = 0.001, *p* = 0.9666	F(1, 8) = 1.691, *p* = 0.2297
PSS	F(1, 12) = 1.256, *p* = 0.284	F(1, 12) = 0.6753, *p* = 0.4272	**F(1, 12) = 10.87, *p* = 0.0064**	**F(1, 8) = 23.00, *p* = 0.0014**
WD	**F(1, 12) = 11.35, *p* = 0.0056**	**F(1, 12) = 11.270, *p* = 0.0057**	F(1, 12) = 1.565, *p* = 0.2348	**F(1, 8) = 8.237, *p* = 0.0208**
CDU vs WDU	*p* = 0.2760	*p* = 0.2500	*p* = 0.7975	*p* = 0.0715
CDU vs CDE	*p* = 0.9885	*p* = 0.7634	*p* = 0.1383	***p* = 0.0110**
CDU vs WDE	***p* = 0.0350**	*p* = 0.3230	***p* = 0.0325**	***p* = 0.0028**
WDU vs CDE	*p* = 0.4198	*p* = 0.0512	*p* = 0.4964	*p* = 0.5539
WDU vs WDE	*p* = 0.5985	*p* = 0.9977	*p* = 0.1523	*p* = 0.1399
CDE vs WDE	*p* = 0.0605	*p* = 0.0700	*p* = 0.8277	*p* = 0.6940

Table 1
Detailed summary of behavioral assessment findings and statistics. Bold denotes significant effects following three-way ANOVA and post hoc comparisons between CD UNEXP, CD EXP, WD UNEXP, and WD EXP. Sample size = 14 rats/group (before outlier testing). Abbreviations: CD control diet, WD western diet, EPM elevated plus maze, SYM Social Y Maze, FPS fear-potentiated startle, ASR Acoustic Startle Reflex, SYM Social Y Maze, UNEXP Unexposed, WD Western Diet.

	ASR	FPS	EPM		SYM	
	(% change from baseline)	(% FPS)	(% OA duration)	(Closed Arm Entries)	(# social interactions)	Frequency (Conspecific: Object)
Source of Variation	F Statistic, posthoc	F Statistic, posthoc	F Statistic, posthoc	F Statistic, posthoc	F Statistic, posthoc	F Statistic, posthoc
WD x PSS	F(1, 51) = 0.204, *p* = 0.6533	F(1, 34) = 0.034, *p* = 0.853	F(1, 52) = 1.731, *p* = 0.1941	F(1, 53) = 0.009, *p* = 0.9229	F(1, 50) = 0.442, *p* = 0.5088	F(1, 47) = 0.065, *p* = 0.7993
PSS	**F(1, 51) = 4.708, *p* = 0.0347**	**F(1, 34) = 7.511, *p* = 0.009**	**F(1, 52) = 4.818, *p* = 0.0326**	F(1, 53) = 0.3639, *p* = 0.5489	**F(1, 50) = 5.293, *p* = 0.0256**	F(1, 47) = 1.664, *p* = 0.2034
WD	**F(1, 51) = 5.305, *p* = 0.0254**	F(1, 34) = 0.008, *p* = 0.927	**F(1, 52) = 15.89, *p* =0.0002**	F(1, 53) = 0.0110, *p* = 0.9167	**F(1, 50) = 5.168, *p* = 0.0273**	**F(1, 47) = 4.180, *p* = 0.0465**
CDU vs WDU	*p* = 0.2306		*p* = 0.2467		*p* = 0.1882	*p* = 0.3829
CDU vs CDE	*p* = 0.6411	*p* = 0.0903	*p* = 0.9281		*p* = 0.1816	*p* = 0.7022
CDU vs WDE	*p* = 0.9997		***p* = 0.0004**		***p* = 0.0134**	*p* = 0.1048
WDU vs CDE	***p* = 0.0105**		*p* = 0.5737		*p* > 0.9999	*p* = 0.9490
WDU vs WDE	*p* = 0.2372	*p* = 0.1530	*p* = 0.0672		*p* = 0.6421	*p* = 0.8809
CDE vs WDE	*p* = 0.5513		***p* = 0.0024**		*p* = 0.6543	*p* = 0.5812

Table 3
Statistical Information on microglial distribution by population phenotype in Fig. 4. A Chi-squared analysis (1982) was performed, and distribution is denoted in number and percentage over three distinct phenotypical distributions. Sample size: Neurohistology: 16,487 *Iba-1*+ cells, 4 rats/group.

	Hyper-ramified	Intermediate	Hypo-ramified
Experimental groups	# *Iba-1*+ | (% population)	# *Iba-1*+, (% population)	# *Iba-1*+, (% population)
WD EXP	1417 | (22)	4392 | (70)	505 | (8)
WD UNEXP	844 | (17)	3587 | (75)	383 | (8)
CD EXP	356 | (12)	1501 | (51)	1064 | (37)
CD UNEXP	349 | (14)	1263 | (52)	826 | (34)

Table 4
Statistical information from endocrine reactivity analysis. Fecal corticosterone metabolites were measured. Bold denotes significant effects following three-way ANOVA and post hoc comparisons. Sample size: *t*-test: CD, $n = 12$, WD $n = 13$; FCM 4 weeks (CDU, $n = 4$; CDE, $n = 4$; WDU, $n = 5$; WDE, $n = 5$). FCM 4 weeks + 1 day (CDU, $n = 4$; CDE, $n = 4$; WDU, $n = 5$; WDE, $n = 5$). FCM 5 weeks + 1 day (CDU, $n = 6$; CDE, $n = 6$; WDU, $n = 7$; WDE, $n = 6$).

	FCM	FCM	FCM
	4 weeks in WD	4 weeks in WD + 1 day after first PSS	5 weeks in WD + 1 day after second PSS
Source of Variation	*t*-test, p	F Statistic, post-hoc	F Statistic, post-hoc
WD vs CD	t (22) = 3.559, ***p* = 0.0018**	–	–
WD x PSS		**F (1, 14) = 5.185, *p* = 0.0390**	F (1, 21) = 1.398, *p* = 0.2502
PSS		**F (1, 14) = 17.96, *p* = 0.0008**	**F (1, 21) = 5.829, *p* = 0.0250**
WD		**F (1, 14) = 10.90, *p* = 0.0052**	F (1, 21) = 0.9038, *p* = 0.3526
CDU vs WDU		***p* = 0.0071**	*p* = 0.4343
CDU vs CDE		*p* = 0.5688	*p* = 0.8274
CDU vs WDE		*p* = 0.9096	*p* = 0.7418
WDU vs CDE		***p* = 0.0005**	*p* = 0.1029
WDU vs WDE		***p* = 0.0012**	*p* = 0.0743
CDE vs WDE		*p* = 0.8856	*p* = 0.9985

Table 5
Statistical information from hippocampal FKBP5 gene expression. Bold denotes significant effects following three-way ANOVA and post hoc comparisons. Sample size: 3 rats/group.

	Fkbp5
	HPC GE
Source of Variation	F Statistic, post-hoc
WD	**F (1, 8) = 21.67, *p* = 0.0016**
PSS	**F (1, 8) = 8.46, *p* = 0.0196**
WD x PSS	F (1, 8) = 0.02, *p* = 0.8879
CDU vs WDU	*p* = 0.0510
CDU vs CDE	*p* = 0.2800
CDU vs WDE	***p* = 0.0030**
WDU vs CDE	*p* = 0.6243
WDU vs WDE	*p* = 0.2139
CDE vs WDE	***p* = 0.0382**

3.1. Exposure to obesogenic conditions during adolescence increases body weight and caloric intake

Body weight and food intake were measured to determine the effects of the obesogenic conditions on growth and caloric intake. We found that WD and PPS promoted significant weight gain. The percent change in body weight after the completion of the stress model (PND81) showed

Table 6
Statistical Information of TNF-α gene expression, protein release and ROS in HCM3 cells following P A + CORT treatment. TNF-α gene expression was significantly affected by the interaction of PA + CORT ($p = 0.0002$) and by CORT treatment alone ($p = 0.0146$). TNF-α protein release was significantly affected by the interaction of P A + CORT ($p = 0.0021$) and by CORT ($p = 0.0002$) and P A ($p = 0.0096$). ROS was significantly influenced by the interaction of P A + CORT ($p = 0.0459$) and by CORT ($p < 0.0001$) and P A ($p < 0.0001$). Bold denotes significant effects following three-way ANOVA and post hoc comparisons. Sample size: gene and protein measurements: 3 rats/group; ROS: 4 rats/group.

	TNF-α	TNF-α	ROS
	Gene expression	Protein release	RFU
Source of Variation	F Statistic, post-hoc	F Statistic, post-hoc	F Statistic, post-hoc
CORT:PA	**F (1, 11) = 30.84, *p* = 0.0002**	**F (1, 12) = 15.19, *p* = 0.0021**	**F (1, 12) = 4.957, p = 0.0459**
CORT	**F (1, 11) = 8.384, *p* = 0.0146**	**F (1, 12) = 28.50, *p* = 0.0002**	**F (1, 12) = 37.02, p < 0.0001**
PA	F (1, 11) = 0.0277, *p* = 0.8706	**F (1, 12) = 9.459, *p* = 0.0096**	**F (1, 12) = 96.35, *p* < 0.0001**
VEH:VEH vs. VEH:PA	***p* = 0.0102**	*p* = 0.9360	***p* = < 0.0001**
VEH:VEH vs. CORT:VEH	*p* = 0.3187	*p* = 0.7415	***p* = 0.0004**
VEH:VEH vs. CORT:P A	*p* = 0.1687	***p* = 0.0003**	***p* = < 0.0001**
VEH:PA vs. CORT: VEH	*p* = 0.2987	*p* = 0.4143	*p* = 0.0878
VEH:PA vs. CORT: PA	***p* = 0.0003**	***p* = 0.0001**	*p* = 0.0755
CORT:VEH vs. CORT:PA	***p* = 0.0114**	***p* = 0.0017**	***p* = 0.0008**

Table 7
Measurements of HCM3 ROS production and M2 polarization following PA + CORT treatment in Fig. 7. Sample size: $n = 4$ rats/group.

	ROS	M1 ROS (−)	M2 ROS (+)
	RFU		
Source of Variation	F Statistic, post-hoc	% ROS	% ROS
VEH	–	73.07	24.40
CORT:PA	**F (1, 12) = 4.957, p = 0.0459**	35.83	62.30
CORT	**F (1, 12) = 37.02, p < 0.0001**	54.93	43.00
PA	**F (1, 12) = 96.35, p < 0.0001**	40.63	56.97
VEH:VEH vs. VEH:PA	***p* = < 0.0001**		
VEH:VEH vs. CORT: VEH	***p* = 0.0004**		
VEH:VEH vs. CORT: PA	***p* = < 0.0001**		
VEH:PA vs. CORT: VEH	*p* = 0.0878		
VEH:PA vs. CORT:PA	*p* = 0.0755		
CORT:VEH vs. CORT: PA	***p* = 0.0008**		

that both WD ($p < 0.0001$) and PSS ($p = 0.0004$) independently contributed to this increase (**S** Fig. 1A). Notably, the combined obesogenic conditions increased weight gain significantly relative to controls ($p < 0.0001$) (**S** Fig. 1A**).** Two-way ANOVA demonstrated that PSS significantly contributed to increased caloric intake ($p = 0.0033$) (S Fig. 1B), suggesting a potential pathway underlying the observed weight gain. Statistical information is detailed in S Tables 2.

Table 8
Statistical Information of Selected gene and protein expression in HCM3 following PA + CORT treatment after FKBP5 SiRNA in Fig. 8. Sample size: $n = 6$ rats/group.

	TNF-α	TNF-α	NF-κB	NF-κB
	Gene expression	Protein release	Gene expression	% Activation
Source of Variation	F Statistic, posthoc	F Statistic, post-hoc	F Statistic, post-hoc	F Statistic, post-hoc
SiRNA	**F (1, 24) = 59.42, $p < 0.0001$**	**F (1, 24) = 16.71, $p = 0.0004$**	**F (1, 24) = 30.54, $p < 0.0001$**	**F (1, 24) = 59.82, $p < 0.0001$**
Treatment	**F (3, 24) = 19.85, $p < 0.0001$**	**F (3, 24) = 3.926, $p = 0.0206$**	**F (3, 24) = 38.97, $p < 0.0001$**	**F (3, 24) = 9.359, $p = 0.0003$**
Treatment: SiRNA	**F (3, 24) = 12.28, $p < 0.0001$**	**F (3, 24) = 7.273, $p = 0.0012$**	**F (3, 24) = 20.54, $p < 0.0001$**	**F (3, 24) = 3.372, $p = 0.0350$**
VEH:Ctrl siRNA vs. VEH: FKBP5 siRNA	***p = 0.0324***	*p = 0.9997*	*p = 0.9998*	*p = 0.3867*
VEH:Ctrl siRNA vs. Cort:Ctrl siRNA	*p = 0.7881*	*p = 0.3417*	*p = 0.6369*	*p = 0.0535*
VEH:Ctrl siRNA vs. Cort: FKBP5 siRNA	***p = 0.0015***	*p > 0.9999*	*p > 0.9999*	*p = 0.9807*
VEH:Ctrl siRNA vs. PA:Ctrl siRNA	***p = 0.0003***	*p = 0.9760*	***p = 0.0045***	***p = 0.0198***
VEH:Ctrl siRNA vs. PA:FKBP5 siRNA	***p = 0.0003***	*p > 0.9999*	*p > 0.9999*	*p = 0.6359*
VEH:Ctrl siRNA vs. PA Cort: Ctrl siRNA	***p = 0.0093***	***p = 0.0004***	***p < 0.0001***	***p = 0.0012***
VEH:Ctrl siRNA vs. PA Cort: FKBP5 siRNA	***p = 0.0031***	*p = 0.9999*	*p = 0.5043*	*p = 0.9995*
VEH:FKBP5 siRNA vs. Cort:Ctrl siRNA	*p = 0.5102*	*p = 0.6236*	*p = 0.8774*	***p = 0.0003***
VEH:FKBP5 siRNA vs. Cort:FKBP5 siRNA	*p = 0.8935*	*p > 0.9999*	*p = 0.9940*	*p = 0.0749*
VEH:FKBP5 siRNA vs. PA: Ctrl siRNA	*p = 0.5498*	*p = 0.9997*	***p = 0.0015***	***p < 0.0001***
VEH:FKBP5 siRNA vs. PA: FKBP5 siRNA	*p = 0.5037*	*p > 0.9999*	*p > 0.9999*	*p = 0.9999*
VEH:FKBP5 siRNA vs. PA Cort:Ctrl siRNA	***p < 0.0001***	***p = 0.0012***	***p < 0.0001***	***p < 0.0001***
VEH:FKBP5 siRNA vs. PA Cort:FKBP5 siRNA	*p = 0.9709*	*p = 0.9838*	*p = 0.2649*	*p = 0.6974*
Cort:Ctrl siRNA vs. Cort: FKBP5 siRNA	*p = 0.0538*	*p = 0.4609*	*p = 0.4506*	*p = 0.3051*
Cort:Ctrl siRNA vs. PA:Ctrl siRNA	***p = 0.0130***	*p = 0.8808*	***p < 0.0001***	*p = 0.9998*
Cort:Ctrl siRNA vs. PA:FKBP5 siRNA	***p = 0.0109***	*p = 0.4224*	*p = 0.7040*	***p = 0.0008***
Cort:Ctrl siRNA vs. PA Cort: Ctrl siRNA	***p = 0.0002***	*p = 0.0818*	***p < 0.0001***	*p = 0.7430*
Cort:Ctrl siRNA vs. PA Cort: FKBP5 siRNA	*p = 0.0997*	*p = 0.1714*	***p = 0.0176***	***p = 0.0169***
Cort:FKBP5 siRNA vs. PA: Ctrl siRNA	*p = 0.9980*	*p = 0.9944*	***p = 0.0094***	*p = 0.1406*
Cort:FKBP5 siRNA vs. PA: FKBP5 siRNA	*p = 0.9960*	*p > 0.9999*	*p = 0.9999*	*p = 0.1687*
Cort:FKBP5 siRNA vs. PA Cort:Ctrl siRNA	***p < 0.0001***	***p = 0.0007***	***p < 0.0001***	***p = 0.0114***
Cort:FKBP5 siRNA vs. PA Cort:FKBP5 siRNA	*p > 0.9999*	*p = 0.9980*	*p = 0.6918*	*p = 0.8308*
PA:Ctrl siRNA vs. PA:FKBP5 siRNA	*p > 0.9999*	*p = 0.9908*	***p = 0.0035***	***p = 0.0003***
PA:Ctrl siRNA vs. PA Cort: Ctrl siRNA	***p < 0.0001***	***p = 0.0040***	***p = 0.0001***	*p = 0.9359*
PA:Ctrl siRNA vs. PA Cort: FKBP5 siRNA	*p = 0.9800*	*p = 0.8601*	*p = 0.3071*	***p = 0.0059***
PA:FKBP5 siRNA vs. PA Cort:Ctrl siRNA	***p < 0.0001***	***p = 0.0006***	***p < 0.0001***	***p < 0.0001***
PA:FKBP5 siRNA vs. PA Cort:FKBP5 siRNA	*p = 0.9694*	*p = 0.9999*	*p = 0.4386*	*p = 0.9017*
PA Cort:Control siRNA vs. PA Cort:FKBP5 siRNA	***p < 0.0001***	***p = 0.0001***	***p < 0.0001***	***p = 0.0003***

3.2. WD and PSS induce distinct effects on cardiometabolic function

Considering the well-documented impact of obesogenic diets and stress on cardiometabolic health, we conducted measurements of fasting blood glucose levels (FBG), heart rate (HR), and blood pressure (BP) at the study endpoint. We found that PSS decreased FBG ($p = 0.0010$), particularly in the rats that consumed the CD ($p = 0.020$) (S Fig. 2). This hypoglycemic response suggests adrenal fatigue and metabolic dysregulation, commonly associated with severe stress. Detailed statistical information can be found in S Tables 2.

Measures of cardiovascular health status showed no significant interactions or main effects of WD or PSS in mean arterial blood pressure (MAP) and systolic blood pressure (SBP). However, the rats that consumed the WD exhibited decreased diastolic blood pressure (DBP) ($p = 0.020$) and heart rate (HR) ($p = 0.0096$) **(S** Fig. 3A–D**)**. In general, although obesity is commonly linked with higher blood pressure, especially SBP, it can paradoxically result in lower DBP and HR in certain individuals, owing to diverse physiological mechanisms. These mechanisms may include expansion of blood volume, increased cardiac output leading to peripheral vasodilation, alterations in adipose tissue-derived hormones influencing vasodilation, changes in renal function affecting fluid balance and sodium handling, and endothelial dysfunction impacting vasomotor tone regulation. Statistical information is detailed in S Tables 3.

3.3. WD intake during adolescence increases the susceptibility to stress-induced anxiety-like behaviors

Previous work from our laboratory and others has demonstrated that exposure to an obesogenic diet during adolescence alters the neural and behavioral substrates implicated with emotional regulation. In this study, we asked whether those effects would be exacerbated when animals are exposed to an obesogenic diet in combination with a robust model of chronic psychosocial stress.

3.4. The obesogenic conditions have differential effects on the acoustic startle reflex maturation

The acoustic startle reflex (ASR) is typically heightened during periods of anxiety and fear in both rats and humans, serving as an indicator of the emotional state of the organism (Koch and Schnitzler, 1997; Grillon and Baas, 2003). In this study, we employed the ASR to group animals and longitudinally evaluate changes in emotional reactivity under obesogenic conditions. Our findings revealed that compared to baseline levels (S Fig. 4A), PSS dampened ($p = 0.035$), whereas the WD elevated ($p = 0.025$), the magnitude of the ASR in adult rats (Fig. 2A). The results of our study highlight significant disparities in the maturation of the startle responsiveness induced by the WD and PSS. Despite controlling for body weight, our findings indicate distinct and contrasting effects exerted by these two factors. Such observations underscore the complex interplay between development, dietary habits, and psychosocial stressors. Table 1 details the *F* stats.

3.5. Exposure to PSS during adolescence increases the magnitude of the fear-potentiated startle

We used the trace fear-potentiated startle (FPS) paradigm to assess hippocampal-dependent conditioned fear learning and fear extinction (Trivedi and Coover, 2006). Our results demonstrated that exposure to PSS significantly increased the FPS during the learning testing session ($p = 0.0097$) (Fig. 2B), supporting sustained enhanced anxiety and fear-related behavior in response to predatory stress (Adamec and Shallow, 1993; Adamec et al., 2006; Zoladz et al., 2015). An interesting observation is that the WD exhibited blunted responsiveness to the aversive footshock (US) compared to CD controls ($p = 0.0007$) (S Fig. 4B). We found a significant interaction effect on FPS responses during the fear extinction testing session ($p = 0.022$) (S Fig. 4C). This indicates that the impact of the WD on fear extinction learning responses is influenced by whether the rats were also exposed to PSS. Specifically, in unexposed rats, the WD diminishes the FPS after fear extinction learning training compared to pre-extinction responses (enhanced fear extinction learning). However, in rats exposed to PSS, the effect of the WD on fear extinction responses is slightly different, with these rats exhibiting a slightly higher FPS (diminished fear extinction learning). It is plausible that stress and dietary factors disrupt fear memory recall in addition to the observed effects on footshock reactivity and fear acquisition. Previous research using delay fear conditioning has examined specific circuit pathways and structural changes that may underlie how the obesogenic diet alters fear responses (Vega-Torres et al., 2018). Statistics are detailed in Table 1.

3.6. WD intake heightens vulnerability to PSS-induced anxiety-like behaviors in the EPM

The elevated plus-maze (EPM) test is widely used to study anxiety-like behavior in rats. We examined EPM behaviors in adult rats after exposure to obesogenic conditions. In agreement with prior findings (Kalyan-Masih et al., 2016), the rats that consumed the WD exhibited a decrease in both the number of entries ($p = 0.0014$) (S Fig. 4D) and the duration spent ($p = 0.0002$) (Fig. 2C) in the open arms. PSS also decreased the duration in the open arms ($p = 0.033$). Evaluation of the total number of closed arms entries as a proxy of motor activity showed no significant difference among all experimental groups (Fig. 2D), indicating that the indices of anxiety observed are unrelated to ambulation. Other ethologically relevant behaviors were measured, and the anxiogenic effect of the WD on the EPM was corroborated (S Fig. 4). For instance, WD rats displayed reduced frequency in the nose dipping zone relative to CD ($p = 0.0002$) (S Fig. 4E). Interestingly, WD consumption significantly reduced the number of stretch attend postures in the EPM ($p < 0.0001$) (S Fig. 4F), a proxy of risk assessment behavior. It is noteworthy that the anxiogenic effect of the WD on these metrics was most pronounced in PSS rats (Table 1 and S Tables 4–5). In summary, these findings collectively support that consuming a WD heightens the manifestation of behavioral indicators of anxiety, particularly in rats exposed to PSS.

3.7. PSS exposure during adolescence reduces indices of sociability

We used the social Y maze to enable observation and evaluation of WD and PSS impact on sociability. We found a significant effect of PSS ($p = 0.026$) and WD ($p = 0.027$) in the total number of social interactions with a caged counterpart (Fig. 2E). Additionally, we observed that the WD rats exhibited a significant reduction in the ratio of interactions between the conspecific and the object ($p = 0.047$) (Fig. 3F), suggesting that the preference was not influenced by the frequency of interactions. PSS reduced the distance traveled during the 9-min test ($p = 0.033$) (S Fig. 4G), which complicated the interpretation of social behavior in the maze. We calculated a sociability index to address this issue that corrected for the total distance traveled. PSS significantly reduced this metric ($p = 0.0060$) (S Fig. 4H). In summary, these results demonstrate that adolescent exposure to an obesogenic that incorporates access to a WD, repeated trauma, and social instability significantly impacts social behaviors in adult rats. A complete report of the statistical details from social behavior assessments can be found in Table 1 and S Table 6.

3.8. Exposure to an obesogenic environment during adolescence leads to microstructural abnormalities in specific hippocampal subfields

The intricate interplay between diet and stress can profoundly affect hippocampal structure(Kalyan-Masih et al., 2016), ultimately shaping behavior through complex neurobiological mechanisms. This study extended our previous research to further elucidate microstructural alterations in hippocampal subfields resulting from adolescent exposure to stress and diet. We used a multimodal imaging approach using magnetic resonance imaging (MRI)-derived diffusion tensor imaging (DTI) and neurite orientation dispersion and density imaging (NODDI) analysis. This novel approach provided detailed characterization of microstructural features within hippocampal subfields and regions, previously inaccessible with conventional imaging techniques. Representative maps of the parameters investigated can be found in S Fig. 5. A comprehensive inventory of descriptive concepts for each parameter is available in S Table 8.

The diffusion tensor model of DTI is based upon three orthogonal axes of diffusion, yielding a diffusivity index from which fractional anisotropy (FA) can be estimated. NODDI distinguishes restricted diffusion in the intracellular compartment, hindered diffusion in the extracellular compartment, and free diffusion in cerebrospinal fluid (CSF), from which parameter maps can be estimated. Fig. 3 shows heatmaps illustrating the impact of the WD and PSS on each neuroimaging metric. We selected the eleven (11) hippocampal subfields and adjacent regions from the atlas. Analyses revealed that FA was significantly altered by the WD ($p < 0.0001$), PSS ($p = 0.0022$), and the interactions between these factors ($p = 0.022$), indicating changes in structural integrity. Mean (M), axial (A), and radial (R) diffusivity indices were also significantly disturbed by the WD (MD: $p = 0.030$) (AD: $p = 0.036$) (RD: $p = 0.028$) and PSS (MD: $p = 0.030$) (AD: $p = 0.033$) (RD: $p = 0.030$). These findings demonstrate restricted water

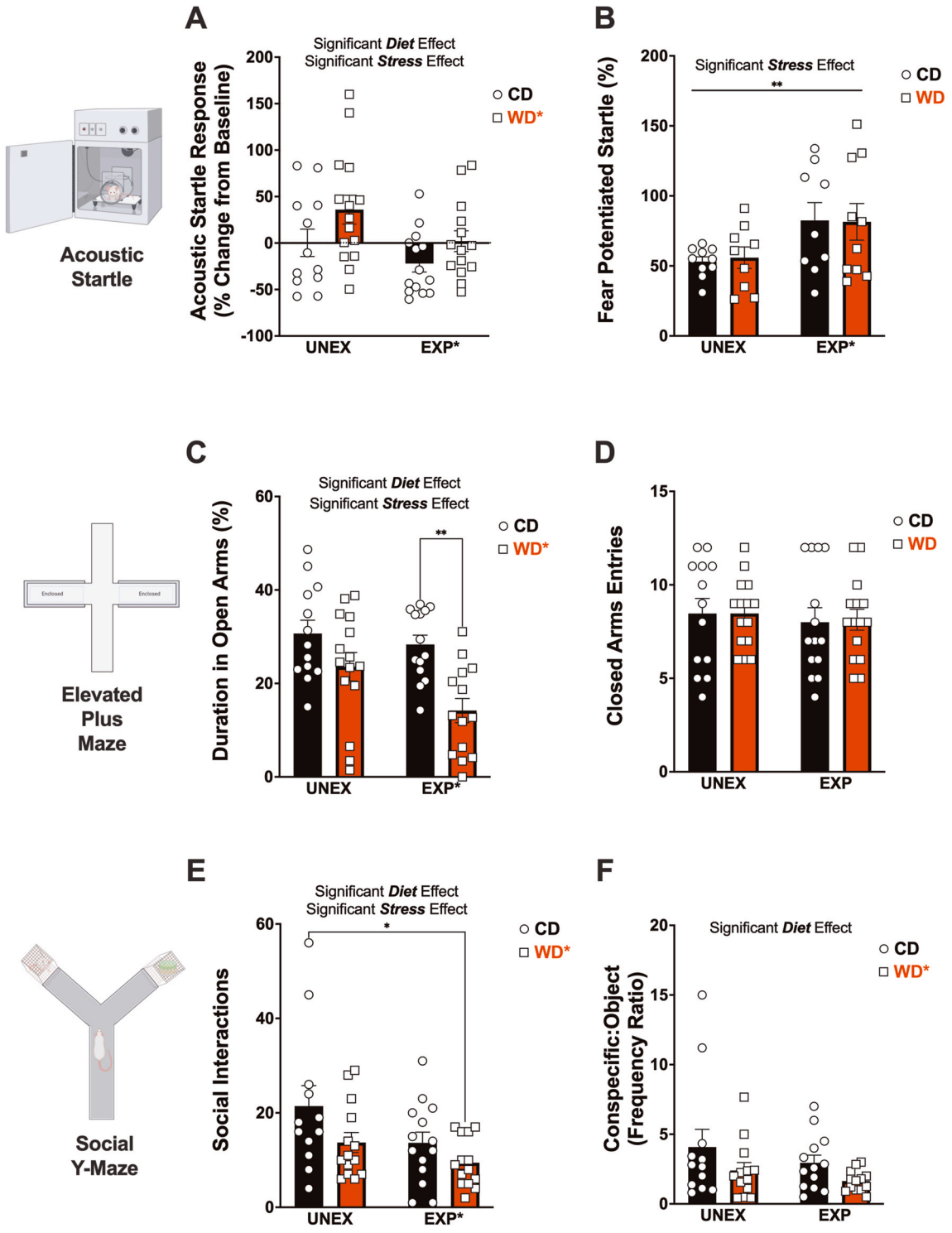

Fig. 2. Adolescent access to an obesogenic diet (WD) and psychosocial stress (PSS) influence startle reactivity, anxiety-like behavior, and indices of sociability. (A) PSS ($p = 0.035$) and WD ($p = 0.025$) had opposing influences on the change in ASR responses from baseline. **(B)** PSS increased the fear-potentiated startle (FPS) ($p = 0.0097$). **(C)** WD consumption ($p = 0.0002$) and PSS exposure ($p = 0.033$) significantly reduce time spent in the open arms of the elevated plus maze. *Post hoc* revealed that WD rats exposed to PSS significantly decreased the time spent in the OA compared to the CD EXP rats ($p = 0.0024$). **(D)** The number of closed arms entries (a proxy of motor activity in the maze) was not affected by the experimental conditions ($p > 0.0050$). **(E)** WD ($p = 0.0273$) and PSS ($p = 0.0256$) reduced the number of social interactions in the social Y-Maze. *Post hoc* revealed that the number of social interactions was robustly decreased by the combined effects of the WD and PSS ($p = 0.0134$ relative to control). **(F)** The WD reduced the frequency ratio of interactions between the conspecific and the object ($p = 0.047$). The sample size for all behavioral tests was 14 rats per group (before outlier testing).

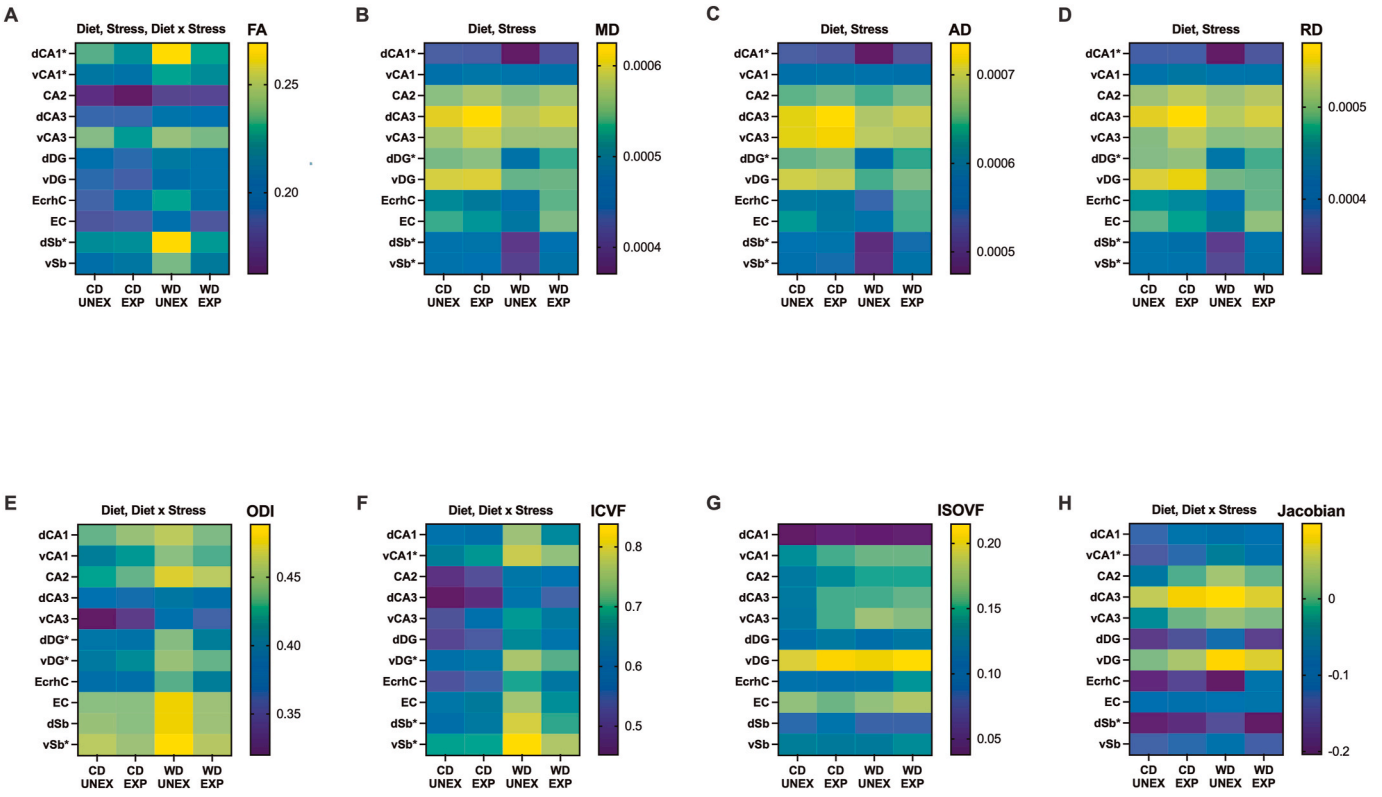

Fig. 3. Exposure to an obesogenic environment during adolescence impacts the structural integrity of distinctive hippocampal subfields, subregions, and adjacent areas. Heatmaps of hippocampal structural changes based on each diffusion-MRI parameter value. **(A)** Fractional anisotropy (FA) was significantly modified by the WD ($p < 0.0001$), PSS ($p = 0.0022$), and the interactions between WD and PSS ($p = 0.022$). **(B–D)** Medial (MD), axial (AD), and radial diffusivity (RD) were also significantly altered by the WD (MD, $p = 0.030$; AD, $p = 0.036$; RD, $p = 0.028$) and PSS (MD, $p = 0.030$; AD, $p = 0.033$; RD, $p = 0.030$). **(E–H)** Orientation dispersion index (ODI), intracellular volume fraction (ICVF), and Jacobian lob matrix data derived from DTI/NODDI analysis revealed that the WD (ODI, $p < 0.0001$; ICVF, $p < 0.0001$; Jacobian, $p = 0.0023$), and WD x PSS ($p = 0.0131$) ($p = 0.0057$) ($p = 0.0270$) significantly contributed to changes in hippocampal tissue integrity. **(G)** The isotropic volume fraction remained unaffected by the experimental conditions. This indicates that changes observed in other DTI metrics are not due to alterations in the overall isotropic volume but may instead reflect changes in tissue microstructure or organization. Asterisks indicate region-specific post hoc effects that significantly contribute to the main and interaction effects observed in the two-way ANOVA (**FA**: dCA1, vCA1; **MD**: dCA1, dDG, vSb; **AD**: dCA1, dDG, dSb, vSb; **RD**: dCA1, dDG, vSb; **ODI**: dDG, vDG, vSb; **ICVF**: vCA1, vDG, dSb, vSb, **Jabobian**: vCA1, dSb). Sample numbers: CD UNEXP, $n = 6$; CD EXP, $n = 7$; WD UNEXP, $n = 8$, WD EXP; $n = 7$. Abbreviations: d, dorsal; v, ventral; CA, Cornu Ammonis, DG, dentate gyrus, EcrhC, ectorhinal cortex; EC, entorhinal cortex; Sb, subiculum; CD, control diet; WD, Western-like diet; UNEX, unexposed; EXP, PSS exposed.

motion due to microstructural alterations. Indices of orientation dispersion, intracellular volume fraction, and Log Jacobian showed to be significantly modified by the WD (orientation dispersion index, ODI: $p < 0.0001$) (intracellular volume fraction, ICVF: $p < 0.0001$) (Jacobian Log: $p = 0.0023$), and interaction effects (ODI: $p = 0.013$) (ICVF: $p = 0.0057$) (Jacobian Log: $p = 0.027$). Analysis shed light on the notable vulnerability of the CA1, dentate gyrus, and subiculum regions to the impacts of diet and stress (see asterisks in Fig. 3 heatmaps). The structural vulnerability noted in these hippocampal subfields may arise from their intricate roles in regulating stress responses and food intake (Jimenez et al., 2018; Bang et al., 2022; Schoenfeld et al., 2019; Davidson et al., 2007). No significant differences were observed in whole-brain volume (interaction: $F_{(1,24)} = 0.92$, $p = 0.35$; stress: $F_{(1,24)} = 3.92$, $p = 0.059$; diet: $F_{(1,24)} = 0.92$, $p = 0.35$), demonstrating that under the conditions tested, diet and stress do not significantly alter total brain volume and that the regional differences were not related to changes in total brain volume. Region-specific details of neuroimaging analyses are found in S Tables 8 and 9

3.9. Adolescent WD and PSS exposure influence hippocampal microglia in adult rats

Microglia are a dynamic population of resident immune cells in the brain responsible for regulating development and maintenance (Paolicelli et al., 2011). Several studies, including ours, reported on microglia's phenotypic and functional heterogeneity under obesogenic conditions (Vega-Torres et al., 2022a). Specifically, our previous multimodal imaging and quantitative microglial morphometric analysis showed a significant response to a short exposure to an obesogenic diet in the CA1 region of the hippocampus (Vega-Torres et al., 2022a). These changes were associated with increased anxiety-like behaviors in rats (Vega-Torres et al., 2022a). Here, we investigated the effects of chronic psychosocial stress and an obesogenic diet in the CA1 hippocampal microglia with a multiparameter quantitative morphometric analysis of Iba1$^+$ cells (Figs. 4 and 5 and S Figs. 7–9).

3.10. WD consumption increases hippocampal microglia cell numbers and promotes a hyper-ramified phenotype

Morphological analyses of 16,250 Iba1$^+$ cells, exploring counts, dimensions, and fractal heterogeneity, revealed precise effects of the WD and PSS on hippocampal CA1 microglia. Representative composite Iba1$^+$ microglial fields (Fig. 4A) and their binarized masks (Fig. 4A') show distinct morphological features analyzed using a FracLac Box Counting Algorithm. In short, grids are systematically scaled over each object (cell) to determine their fractal dimensions (change in pixel value over a spatial pattern). The increase in grid count and complexity allows differentiating cells by morphological features, as shown in

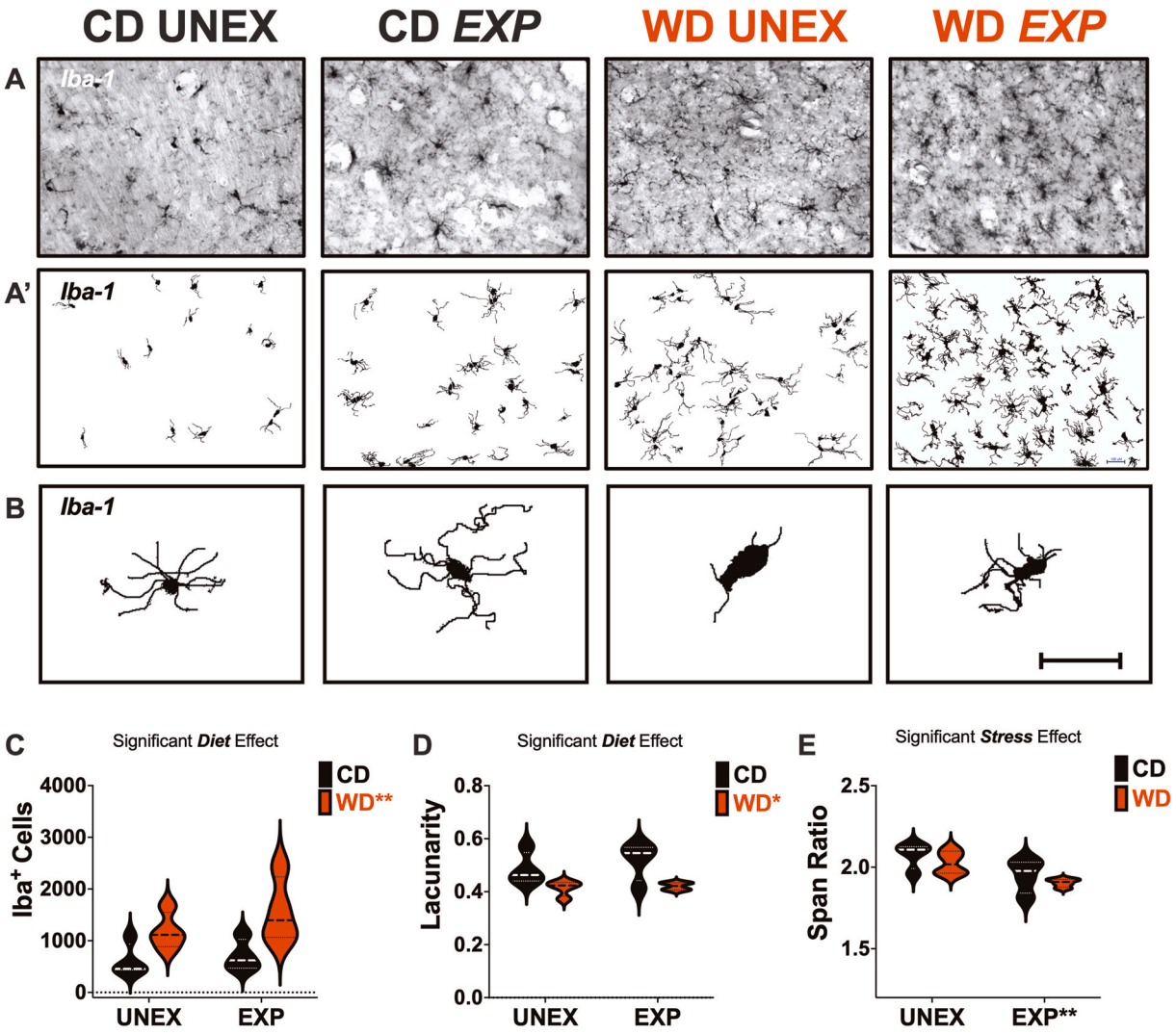

Fig. 4. An obesogenic environment promotes microglial proliferation and proinflammatory morphology in the rat hippocampus. (A) Representative images of full-focused composite 10 × brightfield images from hippocampal CA1 were acquired and stained for Iba-1. **(A′)** Corresponding binarized images were processed for quantitative morphometric analysis. **(B)** Representative microglia morphologies in each study group. **(C)** The WD significantly increased the total Iba1+ cells ($p = 0.0056$). **(D)** Microglial lacunarity was significantly reduced by the WD ($p = 0.0057$). **(E)** Microglial span ratio was significantly reduced in PSS-exposed rats ($p = 0.0064$). Sample size = 4 rats/group. Scale bar for all images: 100 μm.

representative cells for each experimental group (Fig. 4B). Quantifying the total number of Iba1$^+$ cells demonstrated that the WD increased microglial cell numbers in the CA1 ($p = 0.0044$) (Fig. 4C).

Principal component analysis (PCA) was performed to identify morphological features driving group differences. In agreement with prior findings(Vega-Torres et al., 2022b), we identified lacunarity, span ratio, density, and circularity as important differentiating features (S Fig. 7). In agreement with previous reports, we identified lacunarity (form factor) and solidity as the main features impacted by the experimental manipulations. We found that WD significantly decreased lacunarity ($p = 0.033$), a measure of morphological heterogeneity sensitive to changes in particular features such as soma size relative to process length (Fig. 4D). Previous fractal evaluations of microglia morphology have found that lacunarity decreases as the distribution becomes more scattered by the cell cycling to more proinflammatory states (Karperien and Jelinek, 2015). PSS exposure significantly decreased the span ratio ($p = 0.0064$) (Fig. 4E). The span ratio accounts for microglial dimensions and shape and the ratio of the major and minor axes of the outermost points of the cell. Evaluation of microglial density as a measure of cell *solidity* showed that the WD significantly decreased microglial density ($p = 0.029$) (S Fig. 9B) and mean radius ($p = 0.035$) (S Fig. 9C), a measure of cell *roundness*. Circularity describes a biologically relevant shape feature, as it accounts for measures of the ratio of the convex hull area to the perimeter. PSS significantly increased microglial circularity ($p = 0.025$) (S Fig. 9D). These findings prompted us to further investigate relationships between these morphometric parameters to better understand the biology of the microglial responses to PSS and WD.

3.11. An obesogenic environment increases hypo-ramified and intermediate microglia populations in the CA1 subfield of the hippocampus

We used *K*-means clustering to classify cells into three phenotypes based on lacunarity: hyper-ramified, intermediate, and hypo-ramified. The cell distribution in Fig. 5A and S Fig. 8A shows that the WD increased hypo-ramified phenotypes relative to controls (approximately 7% increase). PSS amplified the effect of the WD in expanding this cell population relative to controls (22% vs. 14%). Considering the substantial expansion in intermediate phenotypes induced by the WD (>20% relative to CD), it is probable that the obesogenic conditions prompt a transition into fully hypo-ramified (hyperactive-like) states when combined with PSS (Fig. 5A and S Fig. 8A).

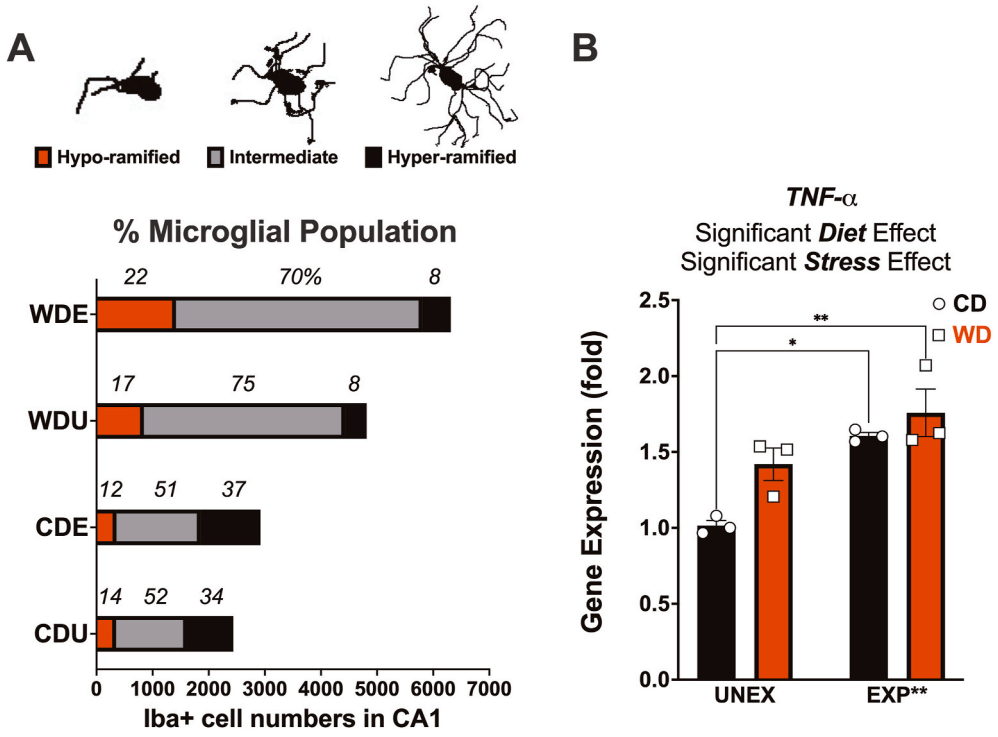

Fig. 5. Obesogenic conditions in adolescence promote significant expansion of 'intermediate' microglia phenotype and TNF-α expression. Principal component analysis (PCA) and *K*-means clustering were used to generate three unique microglial phenotypes based on lacunarity. **(A)** Representative images of the three distinct morphological phenotypes: Hyper-ramified, Intermediate, and Hypo-ramified. The experimental conditions significantly altered the microglial cell distribution based on lacunarity (n, χ^2, df, p; 6,49, 1982, 6, $p < 0.0001$). Hypo-ramified and intermediate phenotypes increased in response to the WD and PSS, while the amount of hyper-ramified cells was reduced. **(B)** Hippocampal TNF-α gene expression was shown to be significantly influenced by both the WD ($p = 0.021$) and PSS ($p = 0.0014$). Relative to UNEX controls, PSS exposure significantly increased hippocampal TNF-α gene expression in CD ($p = 0.0110$) and WD ($p = 0.0028$) fed rats. Sample size: histology: 4 rats/group, 16,487 *Iba-1*+ cells; RT-PCR: 3 rats/group.

We sought to confirm this notion by measuring the mRNA expression of the tumor necrosis factor-alpha (TNF-α) in the hippocampus. In agreement with the morphological findings suggesting a pro-inflammatory/phagocytic phenotype, the WD ($p = 0.021$) and PSS ($p = 0.0014$) increased TNF-α gene expression in the hippocampus. The combination of the obesogenic conditions (PSS and WD) had a robust effect on TNF-α upregulation relative to controls ($p = 0.0028$) (Fig. 5B). Tables 2–3 and S Table 10 detail the microglial morphology statistical measures.

3.12. The obesogenic conditions affect peripheral cytokine levels selectively

Obesity and stress are associated with a marked dysregulation in the circulating levels of several inflammatory mediators that can influence microglia activities. We have shown that dietary high-fat consumption alters cytokine and chemokine profiles in the rat hippocampus and plasma (Vega-Torres et al., 2022b). Building on pflrior observations, we evaluated a panel of thirteen peripheral cytokines using a bead-based flow cytometry immunoassay. Considering the main effects, the WD significantly affected the circulating levels of IL-6 (decreased; $p = 0.012$) and the granulocyte-macrophage colony-stimulating factor GM-CSF (increased; $p = 0.0009$) (S Fig. 12). PSS increased IL1-α levels in plasma ($p = 0.0047$). Notably, the WD and PSS interacted to alter the levels of IL1-α ($p = 0.0033$), IL-10 ($p = 0.018$), GM-CSF ($p = 0.0091$), IL-12p70 ($p = 0.021$), and IL-33 ($p = 0.017$) (S Fig. 12). S Tables 11 and 12 include the results and statistics of the peripheral cytokines tested in this study.

3.13. WD and PSS promote gut microbiota dysbiosis associated with pro-inflammatory microglia and structural neuroadaptations in the hippocampus

Research in both humans and animals demonstrates that disruptions in the gut microbiome can influence neural function and behavior, potentially contributing to the development of various brain disorders. Despite the mechanisms remaining unclear, recent findings highlight the gut microbiota's role in regulating transitions among microglial subtypes (He et al., 2024; Huang et al., 2023). Here, we aimed to investigate the impact of adolescent WD and PSS on gut microbial composition as an initial step toward identifying gut-brain alterations that may influence microglial functions and changes in brain function and behavior. PCA of the unweighted Unifrac distance matrix from the rarefied data was used to evaluate the presence of clusters or groupings based on the operational taxonomic unit (OTU)-level microbial features (S Fig. 10). These analyses indicated that diet type was a significant contributor to their microbial signatures ($p < 0.001$) and discriminated between the two groups regardless of exposure ($p = 0.78$) (S Fig. 10A). Unexpectedly, global parameters of relative bacterial richness ($p = 0.12$) (S Fig. 10B) and diversity ($p = 0.19$) (S Fig. 10C) were similar among groups. Taxonomic classification at the family (S Fig. 10D) and genus (S Fig. 10E) levels showed a selective distribution of *Firmicutes* and *Bacteroidetes* under each experimental condition. The three most abundant families were *Ruminococcaceae*, *Muribaculaceae*, and *Lachnospiraceae*. Interestingly, the relative abundance of *Bacteroidaceae–Prevotellaceae*, a bacterial family associated with the indirect production and transport of secondary metabolites, including short-chain fatty acids (SCFA), was significantly decreased by the exposure to PSS ($p = 0.0040$) (S Fig. 10F). It has been shown that a reduction in SCFAs leads to increased gut permeability(Pérez-Reytor et al., 2021), thus increasing exposure to

bacterial endotoxins and neuroinflammation. SCFAs can also directly influence microglial activities (Erny et al., 2015; Caetano-Silva et al., 2023).

Using PCA, we identified that the relative abundance of three butyrate-producing *Firmicutes—Coprococcus, Ruminococcus, and Lachnospiraceae NK4A136*—were the most important features contributing to the separation between groups under obesogenic conditions. For example, the WD ($p = 0.0033$) and PSS ($p = 0.021$) significantly reduced the relative abundance of *Coprococcus* (Fig. 6A), a bacterium notably depleted in several psychiatric disorders (Nikolova et al., 2021). The obesogenic conditions interacted to affect *Coprococcus* abundance (interaction effect: $p = 0.0052$). The WD also reduced the abundance of *Ruminococcus* ($p = 0.035$) (Fig. 6B), which has been identified as decreased in patients with major depressive disorder (Jiang et al., 2015). We found that the WD ($p = 0.012$) increased while PSS ($p = 0.015$) reduced the abundance of *Lachnospiraceae NK4A136* (Fig. 6C).

Given evidence suggesting that alterations in the abundance or activity of *Lachnospiraceae NK4A136* may influence the effects of stress on gut-brain interactions and overall health, we conducted correlation analyses (Francella et al., 2022; Michels et al., 2019). Spearman's rank correlation coefficient analysis revealed that the abundance of *Lachnospiraceae NK4A136* was inversely correlated with CA1 microglial lacunarity ($r = -0.56$, $p = 0.025$) (Fig. 6D). We also found that *Lachnospiraceae NK4A136* was positively associated with hippocampal fractional anisotropy ($r = 0.617$, $p = 0.012$) (Fig. 6E) and intracellular volume fraction ($r = 0.63$, $p = 0.014$) (Fig. 6F). Similarly, we observed a significant correlation between the abundance of *Bilophila* and the lacunarity of hippocampal microglia ($r = -0.65$, $p = 0.0078$). The expansion of pathobiont bacteria, particularly *Bilophila wadsworthia*, in response to dietary lipids has garnered attention due to its implications for diet-induced inflammation, intestinal barrier function, and metabolic functions (Natividad et al., 2018). Notably, *Bilophila* abundance has also been linked to depressive states (Caso et al., 2021). These results support that obesogenic conditions exert selective adaptive effects on gut microbiome diversity and microbiota remodeling. S Table 11 illustrates additional correlations. Statistical details of microbiome analysis can be found in S Table 13.

The magnitude of the acoustic startle reflexes (ASR) at baseline was correlated with neuroimaging indices in adulthood, including mean diffusivity (MD), radial diffusivity (RD), axial diffusivity (AD), and orientation dispersion index (ODI). Specifically, ASR responses were associated with these neuroimaging parameters (MD: $r = -0.59$, $p = 0.018$; RD: $r = -0.59$, $p = 0.019$; AD: $r = -0.59$, $p = 0.018$; ODI: $r = 0.55$, $p = 0.029$). The observed associations support that structural integrity and connectivity may underlie individual differences in emotionality (Vega-Torres et al., 2018). We identified a negative

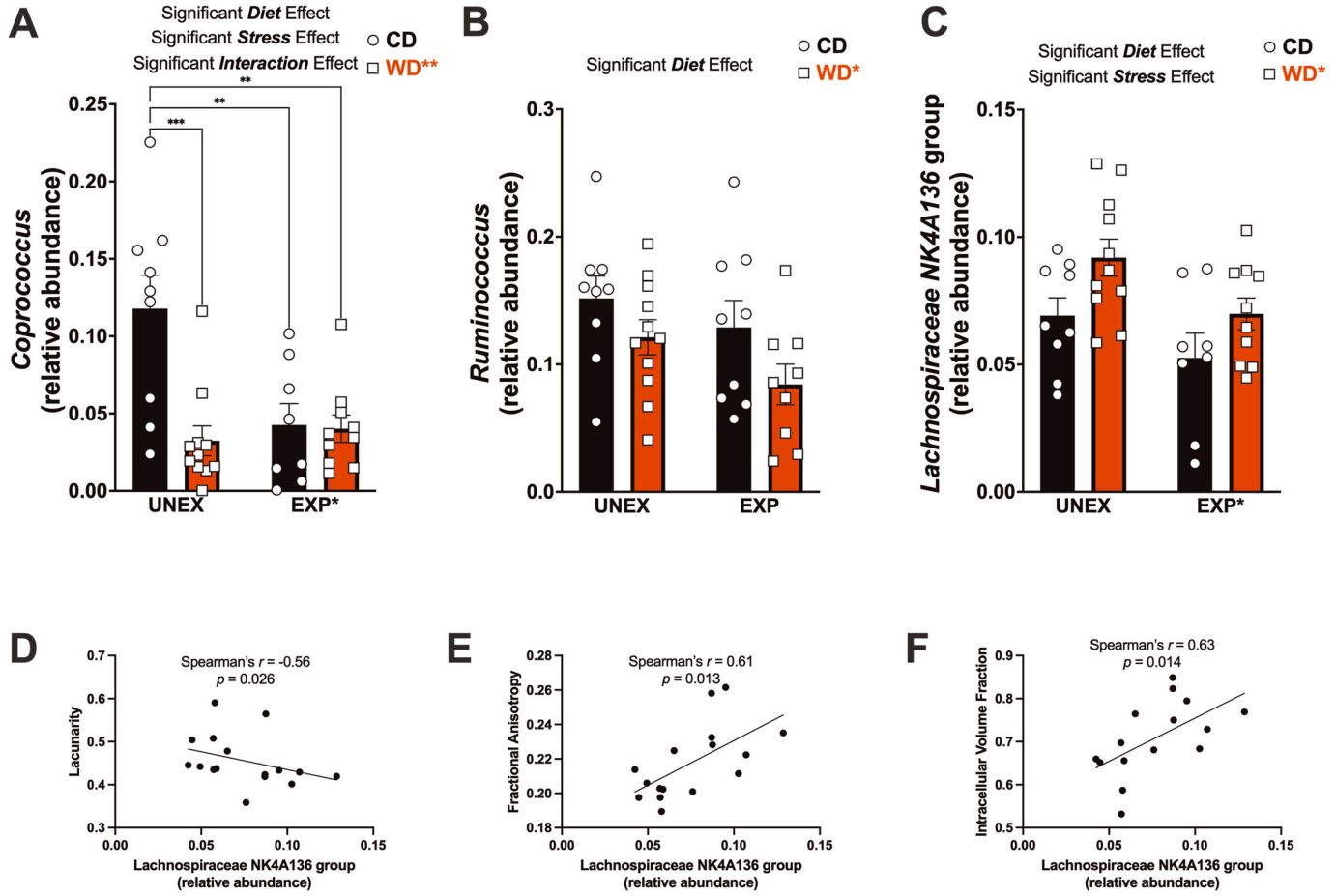

Fig. 6. An obesogenic diet and chronic psychosocial stress induce alterations in *Firmicutes* linked to changes in microglia morphology and brain microstructure. (A) Microbiome evaluation revealed that the WD ($p = 0.0033$), PSS ($p = 0.021$), and interaction of WD and PSS ($p = 0.0052$) significantly contributed to the relative abundance of *Coprococcus* in the gut. Multiple comparisons analysis revealed that, relative to controls, there was a significant reduction in *Coprococcus* abundance due to the WD ($p = 0.0005$), PSS ($p = 0.0048$), and the combined effect of WD and PSS ($p = 0.0019$). **(B)** The WD significantly reduced the abundance of *Ruminococcus* ($p = 0.035$). **(C)** The WD increased ($p = 0.012$), while PSS decreased ($p = 0.015$), the relative abundance of *Lachnospiraceae NK4A136*. Sample numbers: CD UNEXP, $n = 9$; CD EXP, $n = 11$; WD UNEXP, $n = 8$, WD EXP; $n = 10$. Spearman's rank correlation analysis showed significant associations between *Lachnospiraceae NK4A136* abundance and lacunarity **(D)**, fractional anisotropy **(E)**, and intracellular volume fraction **(F)**—correlation sample size = 12 rats. Detailed information on microbiota analyses, correlations, false discoveries, and other related statistics can be found in the Supplementary Materials.

correlation between lacunarity and body weight ($r = -0.62$, $p = 0.012$), further supporting the influence of obesogenic phenotypes on microglial morphology. While no direct links are established, these data validate the interplay between diet, stress, the microbiome, and microglia activities (Erny et al., 2015; Caetano-Silva et al., 2023), which may shape the structure and function of the hippocampus (S Fig. 11). See S Table 14 for statistical details.

3.14. Obesogenic diet and chronic stress influence neuroendocrine stress markers

We sought to evaluate neuroendocrine responses by measuring the primary glucocorticoid in rodents, corticosterone, as metabolites in excreta (fecal corticosterone metabolites, FCM). In male rodents, FCM accounts for 75%–90% of the corticosterone eliminated from the body, with the remainder excreted in the urine. A range of stressors can activate the HPA axis and promote corticosterone release, facilitating prompt adaptation to environmental demands. Chronic adaptive states promote a state of increased allostatic load, which can alter hippocampal plasticity and contribute to the development of neuropsychiatric disorders (McEwen, 2001).

We found that WD intake reduced FCM ($p = 0.0018$) at four weeks of diet consumption (Fig. 7A). The WD ($p = 0.0052$), PSS ($p = 0.0008$), and the interaction between those factors ($p = 0.0039$) were found to significantly influence FCM levels 24 h after the first predator exposure (Fig. 7B). Of importance, only WD rats exhibited increased FCM 24 h after the predator stress exposure relative to unexposed controls ($p = 0.0012$). Predatory stress significantly increased FCM levels at 24 h following the second exposure ($p = 0.025$) (Fig. 7C). Detailed information on statistics can be found in Table 4.

3.15. Obesogenic diet and chronic stress influence hippocampal Fkbp5 gene methylation status at specific sites

The hippocampus plays a pivotal role in terminating the stress response (Bang et al., 2022; Sapolsky et al., 1984; Jacobson and Sapolsky, 1991). Building upon previous investigations conducted by our team (Vega-Torres et al., 2020; Kalyan-Masih et al., 2016), we examined the Fkbp5 gene, which encodes the FK506-binding protein 5—an essential regulator of glucocorticoid activity and acute stress response (Criado-Marrero et al., 2020; Gan et al., 2022; Wagner et al., 2012). Interaction of FKBP5 with intronic regulatory glucocorticoid response elements (GREs) leads to activation and increased transcription. FKBP5 attenuates glucocorticoid signaling via a dynamic process as part of a negative feedback loop. Unexpectedly, we found that both the WD ($p = 0.0016$) and PSS ($p = 0.020$) significantly decreased hippocampal *Fkbp5* mRNA levels at the end of the study (Fig. 7D). Table 5 details the statistics results. The discrepancy with prior studies may be attributed to diet formulation variations and differences in stress intensity and duration (Kalyan-Masih et al., 2016; Balsevich et al., 2014).

Both obesity and traumatic experiences during early life are believed to induce enduring methylation changes in FKBP5 (Womersley et al., 2022; Willmer et al., 2020; Tozzi et al., 2018), (Womersley et al., 2022; Willmer et al., 2020; Tozzi et al., 2018); however, the specific methylation sites involved and the potential interaction between diet and chronic stress in altering epigenetic marks remain poorly understood. We conducted targeted next-generation bisulfite sequencing (tNGBS) from hippocampal samples to identify potential biomarkers for diet and stress responses, evaluating methylation levels across 23 CpG sites in the rat *Fkbp5* gene (S Figs. 14 and 15). Methylation analyses revealed that the WD significantly increased the methylation percent in intron 7 ($p = 0.033$) and intron 8 ($p = 0.024$). PSS led to decreased methylation in the 5′-upstream region ($p < 0.0001$), while it increased methylation in intron 4 ($p = 0.004$) and intron 8 ($p = 0.017$) (Fig. 8). Analyses revealed significant diet × stress interactions in methylation states in the 5′-upstream region ($p = 0.009$), intron 6 ($p = 0.032$), and intron 8 ($p = 0.020$) (Fig. 8). S Tables 16–17 show the detailed statistical analysis. These findings suggest that DNA methylation signatures within *Fkbp5* may serve as potential indicators of the hippocampal response to early obesogenic environments.

3.16. FKBP5 integrates microglial pro-inflammatory signals under obesogenic conditions

Next, we used human-immortalized microglial cell line clone 3 (HMC3) to investigate potential mechanisms linking dietary obesity to stress susceptibility (Russo et al., 2018). HCM3 cells have been extensively characterized with respect to cell morphology, antigenic profile, and cell function, reliably showing most of the original antigenic properties and expressing specific microglial markers. Palmitic acid (PA) is the most abundant free saturated fatty acid in the WD (S Table 1). This fatty acid produces a metabolic, inflammatory response associated with

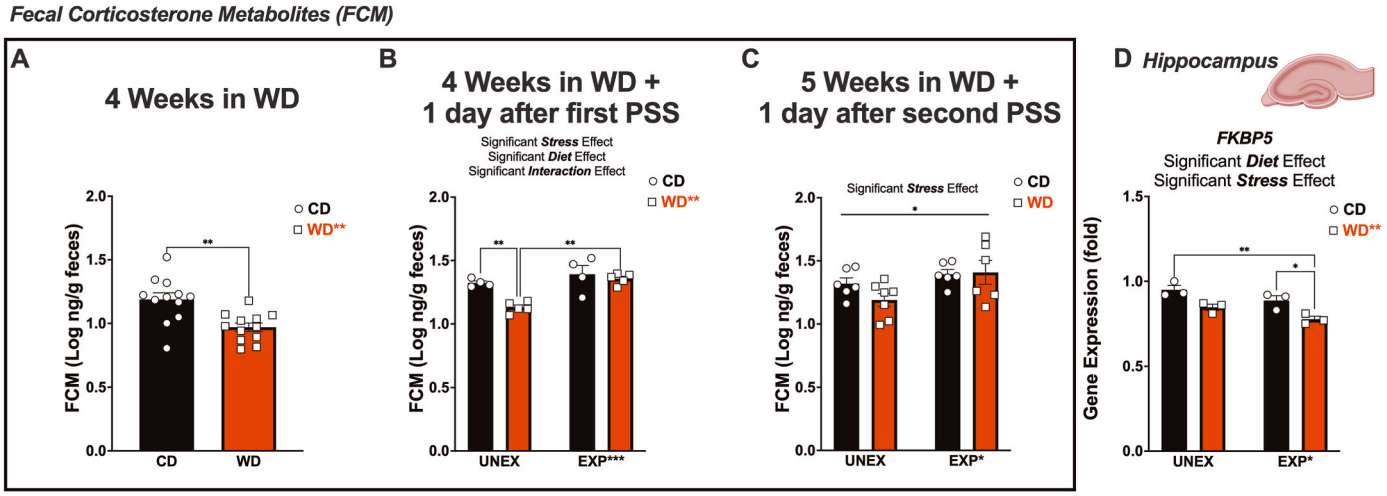

Fig. 7. Exposure to an obesogenic diet and chronic psychosocial stress influence corticosterone levels and hippocampal *Fkbp5* gene expression. (A) Fecal corticosterone metabolite (FCM) levels were significantly decreased by the WD ($p = 0.0018$). **(B)** We observed significant effects of WD ($p = 0.0052$), PSS ($p = 0.0008$), and their interaction ($p = 0.039$) following the first day after predatory exposure. PSS significantly increased FCM levels in the WD rats ($p = 0.0012$). **(C)** FCM remained significantly elevated in PSS rats 24 h after the second predatory exposure ($p = 0.0250$). **(D)** Hippocampal *Fkbp5* mRNA levels were significantly decreased by the WD ($p = 0.0016$) and PSS ($p = 0.020$). RT-PCR: 3 rats/group.

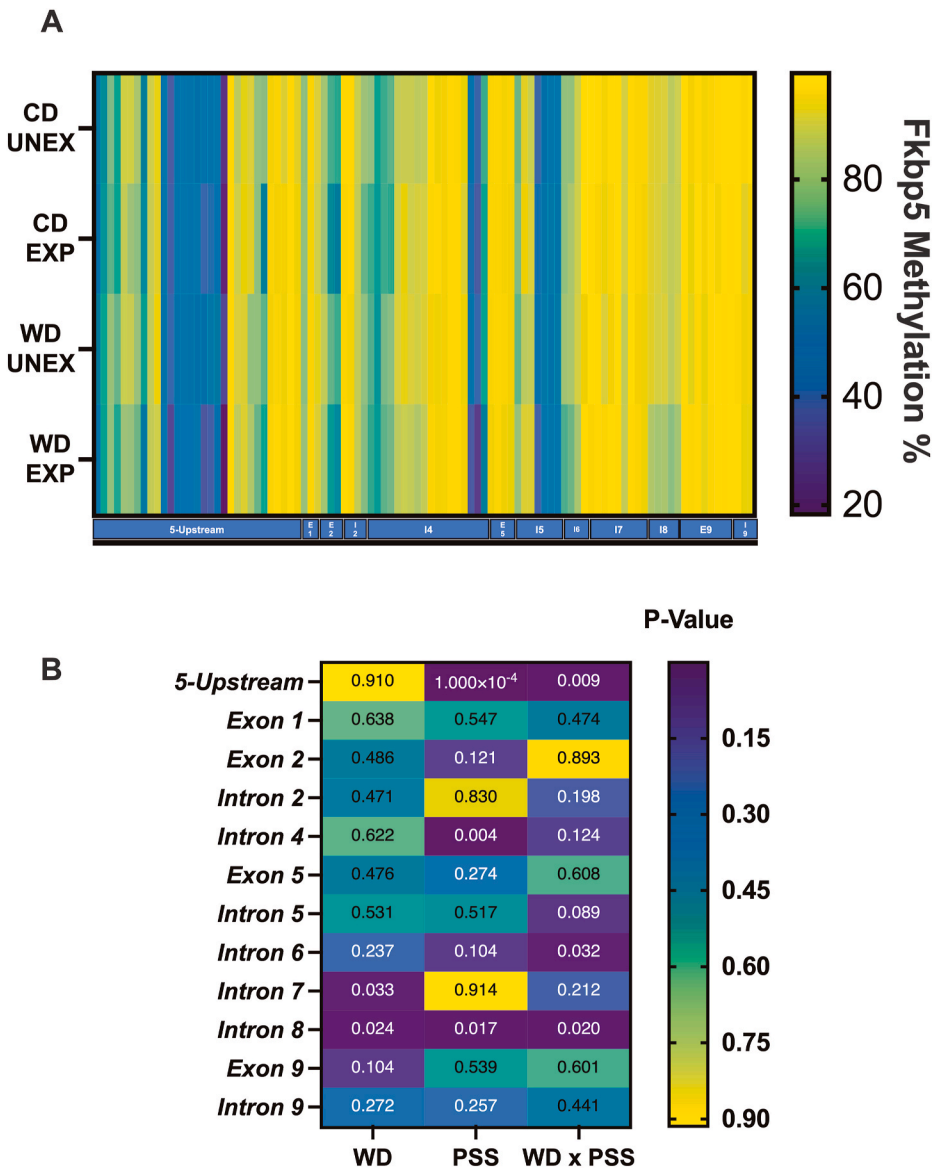

Fig. 8. Heatmap and analysis of rat *Fkbp5* methylation signatures per gene region. (A) Global percentages of *Fkbp5* methylation per locus **(B)** Breakdown of significance per region. Methylation in the 5′-upstream region was significantly modified by PSS ($p = 0.0001$) and the interaction of WD x PPS ($p = 0.009$). Intron 4 was significantly modified by PSS ($p = 0.003$). Intron 6 was modified by WD x PSS ($p = 0.032$). Intron 7 was modified by the diet ($p = 0.032$); Intron 8 was modified by WD ($p = 0.024$), PSS ($p = 0.017$), and WD x PSS (0.024). The summary of statistical values of multiple comparisons in FKBP5 by regions can be found in Supplementary Table 16A–C and 17.

damaging mechanisms such as oxidative stress (Wang et al., 2012b; Lu et al., 2021). We sought to determine whether PA would replicate the dysregulated stress and immune responses observed in our model. HCM3 cells culture and treatment conditions were optimized to determine cell viability and the half-maximal inhibitory concentration (IC_{50}) (S Fig. 16). HCM3 cells treated with increasing concentrations of PA (0–800 μM) showed no significant difference in the percent of viability between cells treated with PA or PA + hydrocortisone (CORT). IC_{50} for PA was determined to be 33.52 μM, and PA + CORT was 50.84 μM. HMC3 cells treated with increasing concentrations of CORT (0–1000 nM) and viability assays showed a 50% of growth inhibition (IC_{50}) at 119.3 nM (S Fig. 16). HMC3 cells were subjected to a dual treatment regimen, mirroring the two-hit rat model. HCM3 cells were primed with PA (50 μM) or vehicle for 24 h, and CORT (100 nM) was added for 24 h (Fig. 9). PA markedly increased cell proliferation after 24 h (Fig. 9A). TNF-α levels are a crucial focus of the stress response and are known to exert potent neuromodulatory effects (Ohgidani et al., 2016; Johnson et al., 2019). To this end, we assessed TNF-α gene expression in the cell lysates and protein levels released in the supernatant. Notably, PA and CORT exhibited an interaction effect on TNF-α gene expression ($p = 0.0002$). While PA alone decreased TNF-α gene expression ($p = 0.010$), pretreatment with PA followed by subsequent CORT treatment robustly increased TNF-α mRNA levels ($p = 0.0003$). (Fig. 9B). Levels of TNF-α protein release were significantly influenced by CORT ($p = 0.0002$), PA ($p = 0.0096$), and the interaction between PA and CORT ($p = 0.0021$) (Fig. 9C). We found that PA + CORT significantly increased secreted TNF-α protein levels relative to control conditions ($p = 0.0003$), supporting the increased mRNA levels. PA and CORT displayed similar effects on IL-6 regulation, as depicted in Figs. S20A–B, implying that these effects may extend to other pro-inflammatory cytokines. Table 6 summarizes the statistics.

During periods of high pro-inflammatory activity, microglia undergo a morphological transformation into an amoeboid shape. In this state, microglia secrete various proteins, including reactive oxygen species

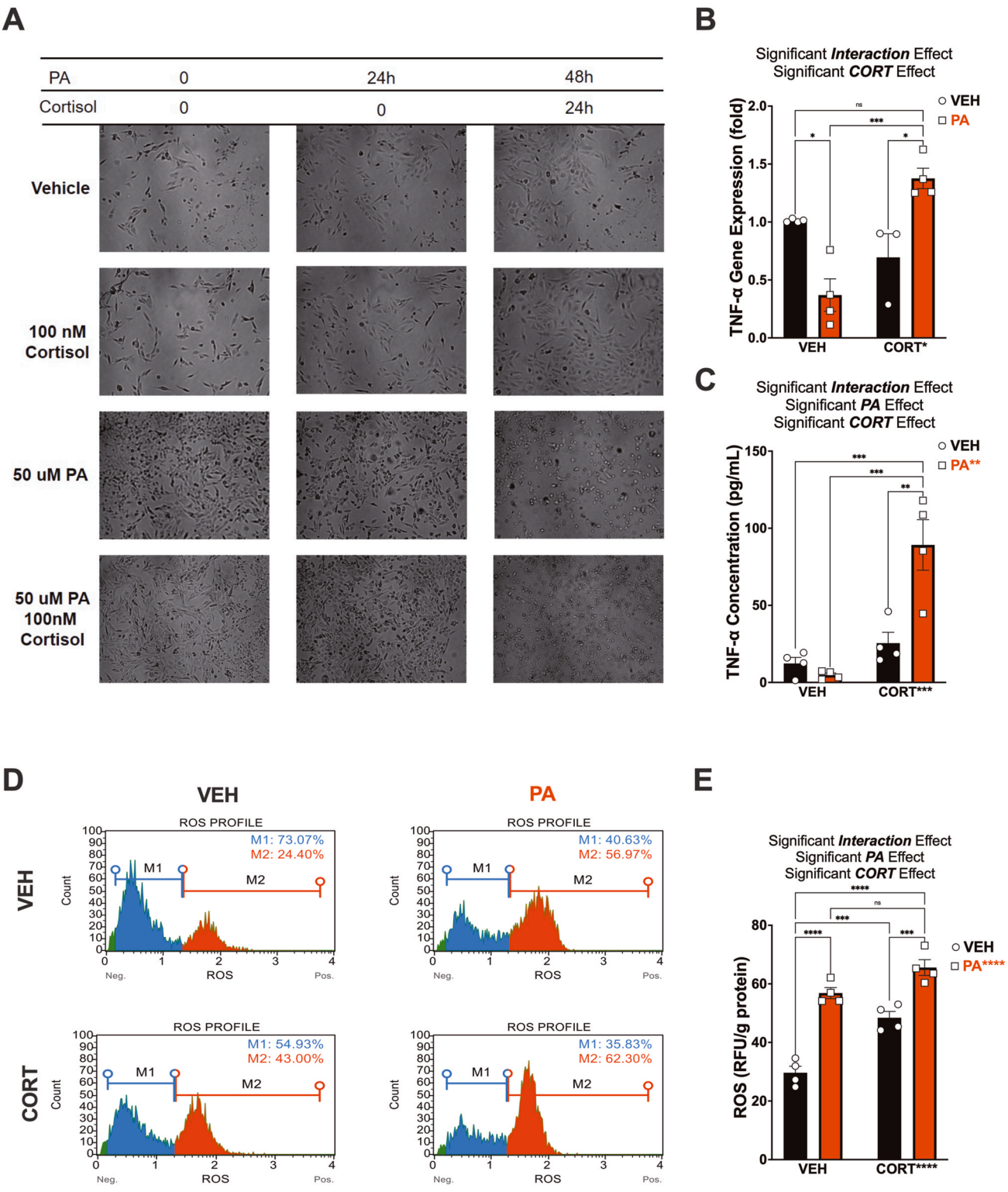

Fig. 9. Palmitic acid sensitizes human microglial cells to abnormal responses to cortisol. (A) Representative brightfield images of human microglial cells (HCM3 cells) pretreated with either vehicle (VEH) or 50 μM palmitic acid (PA), followed by treatment with VEH or 100 nM hydrocortisone (CORT) 24 h later. Cells and supernatant were collected 24 h after CORT/VEH treatment. **(B)** We found an interaction effect on TNF-α mRNA levels ($p = 0.0002$), indicating that the relationship between PA and TNF-α mRNA expression depends on the presence of CORT. Incubation of PA followed by CORT promoted a dramatic increase in TNF-α mRNA expression relative to control conditions ($p = 0.0003$). **(C)** TNF-α protein levels were also significantly influenced by PA ($p = 0.0096$), CORT ($p = 0.0002$), and the interaction of PA x CORT ($p = 0.0021$), partly supporting the mRNA expression results. **(D)** Reactive Oxygen Species (ROS -intracellular superoxide levels) were detected by dihydroethidium (DHE) measurements, showing increased ROS-positive cells after PA (33% increase) and CORT (19% increase) treatment. PA priming resulted in a 38% increase in ROS + cells after CORT treatment (relative to control conditions). M1 = ROS negative cells; M2 = ROS positive cells. PA increased **(E)** Quantification of ROS levels normalized by grams of protein demonstrated a significant ROS increase in PA ($p < 0.0001$) and CORT ($p < 0.0001$) treated cells. We also observed a significant interaction effect ($p = 0.0459$). RFU: relative fluorescence unit. *$p < 0.05$, **$p < 0.01$ and ***$p < 0.001$ ****$p < 0.0001$. Sample size = four independent experiments. Error bars represent standard errors.

(ROS), which can significantly influence synaptic plasticity. Thus, we examined ROS formation under the experimental conditions. ROS was expressed as RFU and normalized to protein levels (Fig. 9D). The levels of ROS were significantly elevated by PA ($p < 0.0001$), CORT ($p < 0.0001$), and by the combination of PA and CORT ($p = 0.046$). It is noteworthy that PA and CORT elevated both the relative abundance of ROS^{+} cells and the levels of ROS ($p < 0.0001$) (Fig. 7D and E). Statistical analyses are detailed in Tables 6 and 7 These results were confirmed via immunofluorescence staining of HCM3 with the phagocytic marker cluster of differentiation 68 (CD68). During homeostasis, the expression of the lysosomal protein CD68 is low in microglia. However, CD68 expression is upregulated in microglia in response to phagocytic activity. Studies have shown that CD68 expression increases in stress-susceptible mice after chronic social defeat stress(Picard et al., 2021), suggesting that microglia become more phagocytic during chronic stress. Cytochemical examination revealed that PA and CORT increased CD68 expression in microglial cells (S Fig. 17). The obesogenic environment caused by priming with PA and subsequent exposure to CORT showed the characteristic morphological changes of microglial activation with enhanced phagocytic activity.

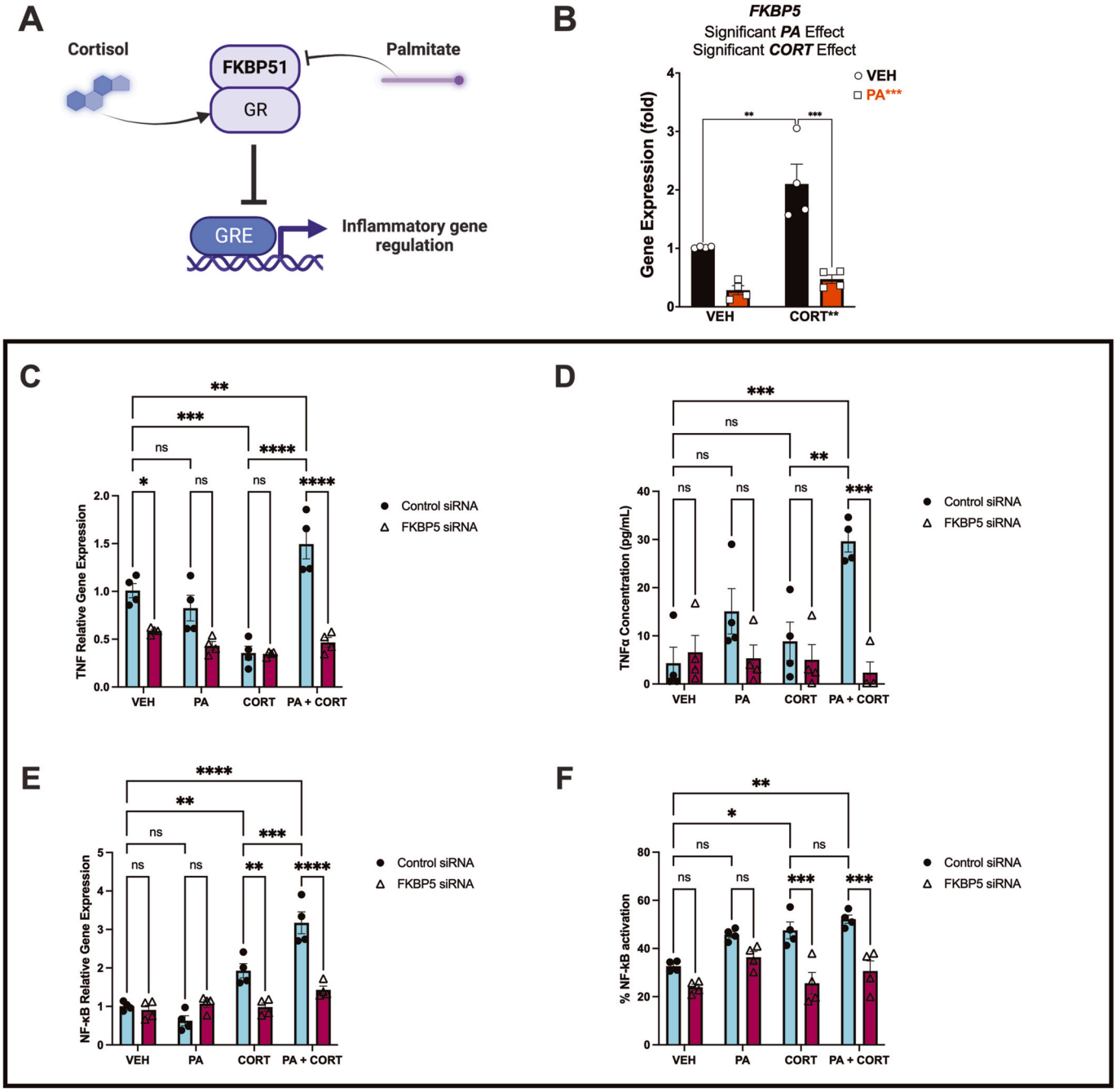

Fig. 10. Human FKBP5 regulates microglial TNF-α levels under obesogenic factors. (A) Schematic model illustrating the primary hypothesis that PA disrupts pro-inflammatory gene expression mediated by the glucocorticoid receptor (GR) through FKBP5/FKBP51 regulation. **(B)** In support of this notion, PA significantly reduced FKBP5 mRNA levels ($p < 0.0001$)—sample size = four independent experiments. FKBP5 siRNA delivery attenuated the impact of PA + CORT on TNF-α upregulation ($p < 0.0001$) **(C)** and released protein levels of TNF-α ($p = 0.0001$) **(D)**. CORT increased NF-κB gene expression **(E)** and protein activation ($p < 0.05$) **(F)**. This effect was reduced in cells treated with FKBP5 siRNA ($p < 0.001$) **(E-F)**—sample size = four independent experiments.

3.17. FKBP5 plays a crucial role in microglial immunometabolic regulation

Dietary obesity-induced inflammation has the potential to impact neuroendocrine function, neurotransmitter metabolism, regional brain activity, and, ultimately, behavior. Emerging studies demonstrate that FKBP51/FKBP5 is involved in these responses (Gan et al., 2022). Thus, we tested the hypothesis that palmitic acid (PA) disrupts FKBP5-mediated pro-inflammatory gene transcription (Fig. 10A). First, we examined the influence of hydrocortisone (CORT) on FKBP5 mRNA levels in HCM3 cells. We found that cells treated with increasing concentrations of CORT (0–1000 nM) showed a U-shaped response in FKBP5 expression (S Fig. 18). Next, we investigated how PA-induced priming affects the expression of FKBP5 mRNA levels mediated by CORT. We found that FKBP5 gene expression was significantly decreased by PA ($p < 0.0001$), CORT ($p = 0.0038$), and PA + CORT ($p = 0.028$) (Fig. 10B), which is partly consistent with the findings from rat hippocampal tissue (Fig. 7D and S Fig. 19). CORT treatment significantly increased FKBP5 expression ($p = 0.0049$), and PA pretreatment in CORT-treated cells showed a blunted expression of FKBP5 ($p = 0.0002$) (Fig. 10B).

To investigate the role of FKBP5 further in integrating immune responses to PA and CORT, we used small interfering RNA (siRNA) to silence FKBP5. We evaluated the response and activation of essential microglial pathways involved in the immunoregulation of the stress response (Ohgidani et al., 2016; Kemp et al., 2022). We discovered that TNF-α mRNA levels were significantly impacted by all experimental conditions, and we identified a significant interaction between treatment and siRNA ($p < 0.0001$) (Fig. 10C). Despite CORT reducing TNF-α mRNA levels in microglial cells, our findings revealed that pre-treatment with PA led to an elevation in TNF-α mRNA levels upon application of CORT. Importantly, we observed that this effect relied on FKBP5, as the silencing with FKBP5 siRNA abolished this response. Likewise, our data uncovered that the combination of PA and CORT led to an augmentation in TNF-α release, a response that was contingent upon the presence of FKBP5 (treatment × siRNA interaction: $p = 0.0012$, treatment: $p = 0.021$, and siRNA: $p = 0.0004$) (Fig. 10D). Cytokines belonging to the TNF family prompt swift transcription of genes that regulate inflammation, cell survival, proliferation, and differentiation. This process is primarily facilitated through the activation of the NF-κB pathway. Our results revealed that CORT heightened NF-κB gene expression, an effect that was significantly potentiated following pre-treatment with PA (significant treatment × siRNA interaction, treatment, and siRNA effects; for all $p < 0.0001$) (Fig. 10E). NF-κB activation was also significantly influenced by treatment + siRNA interaction ($p = 0.035$), treatment ($p = 0.0003$), and siRNA ($p < 0.0001$) (Fig. 10F). Partially aligning with the expression data, both CORT treatment and PA combined with CORT led to heightened NF-κB activation compared to vehicle controls ($p < 0.05$). Consistent with previous research findings (Erlejman et al., 2014; Kästle et al., 2018), we observed that the influence of CORT on NF-κB expression and activation was contingent upon FKBP5, as demonstrated by the blocking effect of the siRNA. The regulatory influence of FKBP5 on cytokine expression and release extended to IL-6 (see S Fig. 20C and D). These findings illustrate the critical involvement of FKBP5 in regulating immune responses in microglia. Table 8 shows the statistical details of these analyses.

4. Discussion

Despite the high comorbidity between obesity and stress-related mental disorders, the pathways contributing to this bidirectional association remain relatively unexplored. This study investigated the biological underpinnings of early exposure to an obesogenic environment characterized by access to an obesogenic diet and chronic psychosocial stress. The main findings are as follows: **1)** we demonstrate that chronic psychosocial stress leads to increased food intake and weight gain, **2)** early exposure to an obesogenic diet and exposure to psychosocial stress impair social behaviors while increasing fear and anxiety-like behaviors, **3)** the obesogenic conditions altered the structural integrity within specific hippocampal formation regions and subfields, **4)** these conditions were associated with significant shifts in gut microbiome distribution, neuroinflammation, and immunometabolic alterations, **5)** mechanistically, we identified the corticosterone receptor chaperone gene FKBP5, as a potential molecular link connecting obesogenic conditions to altered inflammation and stress reactivity. This study identifies novel mechanisms and adaptations by which obesogenic environments shape the maturational trajectories of common neurobiological correlates of stress resilience.

Psychosocial stress is a prevalent environmental factor that contributes to the development of obesity (Perkonigg et al., 2009; McLaughlin et al., 2013; Imperatori et al., 2016; Caslini et al., 2016; Danese and Tan, 2014; Land et al., 2014; Wang et al., 2001; Kohl et al., 2019; Lowe et al., 2019). On the other hand, mounting evidence supports that obesity and metabolic disorders may confer vulnerability to stress-related disorders (Vega-Torres et al., 2018; Kalyan-Masih et al., 2016; Masodkar et al., 2016; Lopresti and Drummond, 2013). The findings presented herein support that obesity predisposes individuals to stress-related complications. Consumption of foods rich in saturated fats and refined sugars has been strongly correlated with the modulation of emotional states. While highly palatable foods can relieve negative emotions by dampening perceived stress in animals and humans, these effects are temporary and pose a risk for increased consumption, obesity, and heightened vulnerability to depression and anxiety (Ulrich-Lai et al., 2015).

Using acoustic and fear-potentiated startle paradigms offers valuable insights into the nuanced relationship between stress responsivity, learning, and emotionality states. Consistent with previous studies, we found that the obesogenic Western diet (WD) augmented proxies of anxiety and blunted the acoustic startle reflex (Kalyan-Masih et al., 2016). Interestingly, PSS reduced the magnitude of the acoustic startle. While anxiety typically involves heightened arousal and vigilance in response to perceived threats, a blunted startle reflex may indicate a dampened physiological response to sudden or intense stimuli. This paradoxical relationship can arise from various factors, including dysregulation of stress response systems such as the hypothalamic-pituitary-adrenal (HPA) axis. For example, chronic exposure to stressors or prolonged activation of stress pathways may lead to desensitization or downregulation of stress response mechanisms, resulting in a blunted startle reflex despite ongoing feelings of anxiety. Studies have documented diminished ASR in individuals diagnosed with post-traumatic stress disorder (Ornitz and Pynoos, 1989; Medina et al., 2001). As previously discussed(Kalyan-Masih et al., 2016), the blunted startle reactivity may suggest sensory thresholds, motor impairments, and peripheral mechanisms alterations. Individual differences in stress sensitivity, coping strategies, and environmental factors can also contribute to the complex interplay between anxiety, fear, and startle responses. Therefore, while seemingly contradictory, the coexistence of heightened fear and a blunted acoustic startle reflex underscores the intricate and nuanced nature of acoustic startle plasticity. Considering the observed effects on responsiveness to a startling stimulus, it might be tempting to attribute these differences to variations in body weight among the experimental groups. However, we must emphasize that we corrected the startle magnitude measurements to account for body weight variations across subjects. This meticulous approach ensured that any observed differences were not attributed to body weight discrepancies. Despite the lack of negative impact on hippocampal-dependent fear learning within the fear-potentiated startle paradigm by WD, our observations demonstrate a potential facilitation of fear extinction learning associated with the WD. This observed response is likely explained by the reduced footshock reactivity observed in rats consuming the WD.

Furthermore, our investigation revealed notable effects on social

behavior stemming from both the WD and PSS. Specifically, rats subjected to these conditions exhibited alterations in their social interactions compared to control groups (even after normalizing for total ambulation). These findings underscore the significant influence of dietary and environmental factors on the adolescent brain and corroborate a substantial body of research demonstrating that an obesogenic environment can impact the maturational trajectories of social behavior by influencing inflammatory and neuroendocrine pathways (Pohl et al., 2014; Vidal et al., 2007).

Neuroimaging has been instrumental in identifying neuropathological changes brought about by obesity and stress. Building upon our previous research (Vega-Torres et al., 2022b; Kalyan-Masih et al., 2016), we discovered that the microstructural integrity of the CA1, dentate gyrus, and subiculum regions was susceptible to the influence of the obesogenic environment. The observed vulnerability of these hippocampal subfields may stem from their intricate involvement in stress response regulation, neurogenesis, and synaptic plasticity. The CA1 region, recognized for its pivotal role in conditioned fear, stress responses, anxiety-related behavior (Jimenez et al., 2018), and food intake (Kosugi et al., 2021), could be particularly sensitive due to its high density of glucocorticoid receptors (Herman et al., 1989). This renders it susceptible to memory impairments (Bakoyiannis et al., 2024), which could be linked to deficiencies in synaptic plasticity and long-term potentiation induced by obesogenic environments. Likewise, the dentate gyrus, a hub for adult neurogenesis, may be impacted by the interplay of diet and stress through the modulation of neurotrophic factors and inflammatory pathways. Changes in neurogenesis within the dentate gyrus have been implicated in mood regulation and stress resilience(Workman et al., 2016; Kreisel et al., 2014), suggesting potential implications for mood disorders and cognitive impairments. The subiculum, acting as a pivotal relay between the hippocampus and other brain regions involved in stress processing, may also be vulnerable to diet-stress interactions. Dysregulation of subicular activity has been associated with alterations in stress hormone release and disruptions in HPA axis feedback mechanisms(Herman et al., 1998), contributing to maladaptive stress responses. The reduction in corticosterone levels in response to the obesogenic diet and the heightened stress reactivity in response to acute predatory stress support this notion. The susceptibility of these hippocampal regions to the combined effects of diet and stress may result in a range of emotional disturbances, as observed in this study, such as increased anxiety and fear-related responses. Despite the apparent opposite effects of diet and stress on hippocampal structure, the combined impact of these factors on rat behavior may result from divergent molecular pathways, compensatory mechanisms, differential effects on hippocampal subregions, or altered neurotransmitter systems. These factors could lead to heterogeneous structural changes, such as neuroinflammation or region-specific plasticity, which may collectively exacerbate behavioral deficits while producing seemingly contradictory structural outcomes. This finding aligns with prior work from our group, which also revealed opposing effects of the WD when combined with psychogenic stress on hippocampal metrics.

Emerging evidence indicates that neuroinflammation significantly contributes to the etiology of stress-related psychiatric disorders (Haroon et al., 2018; Osimo et al., 2020; Felger, 2018). Neuroinflammation encompasses intricate interactions among psychological, neuroendocrine, and nervous systems, leading to alterations in neurotransmitter metabolism, dysregulation of the hypothalamic-pituitary-adrenal axis, pathological activation of microglial cells, compromised neuroplasticity, and structural and functional changes in the brain that impact emotional behavior. Microglia actively participate in brain remodeling processes during both developmental and adulthood stages (Guedes et al., 2022). Emerging research suggests that the maturation and function of selected neurocircuits may be regulated by the molecular identity that microglia adopt on different regions in the brain (Guedes et al., 2022). Given the increased sensing ability of microglia to diet and stress cues, defective microglia may significantly contribute to the function and maturation of the neurocircuitries affected by obesogenic environments (Cope et al., 2018; Calcia et al., 2016). Our findings align with previous research that highlights the significant impact of early-life stress (ELS) on neurodevelopment through stress-induced neuroinflammation. Frances and Kaffman (2018) (Johnson and Kaffman, 2018) and Reemst et al. (2022) (Reemst et al., 2022) have shown that ELS disrupts microglial morphology, gene expression, and phagocytic capacity in the hippocampus during critical periods of brain development, leading to lasting behavioral effects. In our study, the WD and PSS induced significant alterations in microglial morphology, affecting cell counts, dimensions, and fractal heterogeneity. Specifically, WD increased microglial cell numbers and decreased lacunarity, indicating a shift toward a pro-inflammatory phenotype. At the same time, PSS altered the span ratio and increased circularity, reflecting a morphological shift toward an “activated” state. These morphological changes were further corroborated by the upregulation of TNF-α expression in the hippocampus, particularly under combined obesogenic conditions. Our results suggest that WD and PSS contribute to neuroinflammatory processes and promote a transition of microglia to a more pro-inflammatory state. This transition potentially mirrors the effects of ELS on critical neurodevelopmental processes, such as synaptogenesis, synaptic pruning, axonal growth, and myelination, leading to behavioral abnormalities that persist into adulthood. Given the complexity and limited understanding of the underlying molecular mechanisms, our studies highlight the importance of focusing on morphological outcomes as sensitive indicators of microglial changes in response to obesogenic diets. These morphological metrics reveal dynamic microglial activities, offering a more direct measure of microglial responses critical to understanding synaptic remodeling and the broader brain structure in obesity.

One potential pathway through which obesity could impact brain and behavioral responses to stress is altering the microorganisms within the gastrointestinal tract. The gut microbiome is critical to digestion, metabolism, immune system development, brain function, and other host physiological functions (Margolis et al., 2021; Mayer et al., 2015). Obesity and associated dietary patterns result in marked and persistent gut microbiome composition and diversity alterations (Wit et al., 2023; Xu et al., 2022; Wu et al., 2011). Microbial imbalances or dysbiosis can lead to alterations in brain permeability (Margolis et al., 2021), potentially contributing to (neuro)inflammation and maladaptive stress responses (Rea et al., 2016). Dysbiosis can lead to a "leaky gut," allowing bacterial products such as lipopolysaccharides (LPS) to enter the bloodstream, triggering systemic inflammation that weakens the blood-brain barrier (BBB). This enables pro-inflammatory cytokines and immune cells to infiltrate the brain, activating microglia and perpetuating neuroinflammation. The resulting oxidative stress further exacerbates inflammation and compromises microglia, disrupting brain maturation. The gut microbiome plays a crucial role in neural development (Socała et al., 2021). Furthermore, elevated levels of bacterial metabolites, pro-inflammatory mediators, and exposure to environmental stress can activate microglia, potentially influencing behavior (He et al., 2024; Reyes et al., 2020; Lynch et al., 2021). We found that the obesogenic diet and stress reduced the abundance of short-chain fatty acid (SCFA)-producing bacteria, which can increase gut permeability(Pérez-Reytor et al., 2021), thus increasing exposure to bacterial endotoxins that promote neuroinflammation. SCFAs can also directly influence microglial activities (Erny et al., 2015; Caetano-Silva et al., 2023). In particular, psychosocial stress reduced the relative abundance of the *Firmicutes*, *Lachnospiraceae NK4A136*. Emerging research indicates that changes in the abundance or activity of *Lachnospiraceae NK4A136* could mediate the impacts of stress on gut-brain interactions and overall health (Francella et al., 2022; Michels et al., 2019). Further investigation into the specific mechanisms and functional roles of *Lachnospiraceae NK4A136* is warranted to understand its contributions to stress-related responses. Although the causal relationships between early obesogenic environment exposure and stress-susceptibility are

unclear, this study expands on the increasing number of reports of studies in animals and humans that link the ontogeny and pathology of stress-related disorders to the microbiome composition.

Both diet and stress exert profound effects on microglial functions through epigenetic mechanisms. Epigenetic modifications, such as changes in DNA methylation and histone acetylation, can alter gene expression patterns in microglia in response to environmental cues. One potential mechanism involves the FKBP5 gene, which is crucial in regulating the stress response. FKBP5 is a critical regulator of the glucocorticoid receptor pathway, which is highly relevant in the context of stress-induced neuroinflammatory processes. Given its centrality in linking stress to immune responses, particularly in microglia, it offers a specific and mechanistically insightful target for understanding how stress influences neuroinflammation. We present new evidence that an obesogenic diet can prime microglia for aberrant immune responses to stress, leading to a hyper-engulfing phenotype that may disrupt synaptic integrity and hippocampal circuits, potentially contributing to anxiety. Influenced by environmental factors, epigenetic changes can modulate the effects of allele-specific variants in the FKBP5 gene (Häusl et al., 2019; Criado-Marrero et al., 2020; Balsevich et al., 2014; Schmidt et al., 2015), (Häusl et al., 2019; Criado-Marrero et al., 2020; Balsevich et al., 2014; Schmidt et al., 2015), impacting the response to glucocorticoids (GCs) and stress susceptibility (Binder et al., 2004, 2008; Yehuda et al., 2016). We found that the obesogenic conditions shifted the methylation status at CpG sites within and proximal to glucocorticoid response elements (GREs) and other critical regulatory sites(Yusupov et al., 2023), suggesting potential functional relevance. FKBP5/FKBP51 influences microglia activities (Gan et al., 2022) and overall hippocampal structure and function (Córdova-Palomera et al., 2017; Fani et al., 2013; Zobel et al., 2010). Therefore, FKBP5/FKBP51 may predispose individuals with obesity to stress-related psychopathology through its regulation of microglia and maintenance of hippocampal structural integrity. Obesity may imprint long-standing demethylation patterns in microglial FKBP5, leading to chronically dysregulated immunometabolic feedback.

By emphasizing the different exposure durations to palmitic acid (PA) and corticosterone (CORT) in the two settings—chronic exposure *in vivo* versus acute exposure *in vitro*—we highlight how these temporal differences likely influence gene expression outcomes. This distinction is critical, as it acknowledges the complexity of translating findings from controlled cell culture models to the more dynamic *in vivo* environment, where prolonged dietary and stress exposures can have cumulative effects. Furthermore, other hippocampal cell types, beyond microglia, may contribute to the overall expression profiles observed in hippocampal tissue. This underscores the multifaceted nature of neuroinflammatory responses in the brain, where interactions between different cell types can modulate the effects of stress and diet on FKBP5 and TNF-α expression. The inclusion of siRNA experiments further strengthens our argument by directly demonstrating the necessity of FKBP5 in regulating microglial neuroinflammatory responses within the specific context of obesogenic conditions. This evidence supports the hypothesis that FKBP5 plays a crucial role in mediating the effects of a Western diet and stress on neuroinflammation. Overall, this response enhances the rigor and depth of our study, providing a more nuanced understanding of the FKBP5-dependent mechanisms underlying neuroinflammation. We conclude that the interplay between diet, stress, epigenetics, and hippocampal FKBP5 gene regulation may contribute to the pathophysiology of stress disorders in individuals exposed to obesogenic environments during adolescence.

5. Limitations and future studies

In this study, we aimed to assess the brain, behavior, and immunometabolic responses to an obesogenic environment in rats. Initially, we hypothesized that the consumption of an obesogenic diet during adolescence would exacerbate the adverse effects of psychosocial stress on the brain and behavior. However, several limitations should be considered. Firstly, the exclusion of female rats limits the generalizability of our findings, given known sex differences in stress responses observed in humans. An explanation for this initial choice is outlined in the Materials and Methods section. Including female rats in future studies would allow for a comprehensive examination of sex-specific effects. Secondly, while we focused on microglia morphological alterations in the hippocampus, other brain regions and circuits implicated in anxiety and stress-related disorders were not fully characterized. Expanding our investigation to include a broader range of stressors, brain regions, and circuits would provide a more comprehensive understanding of the neurobiological mechanisms involved. Additionally, while our data supports the involvement of *Fkbp5* in stress predisposition within our *in vivo* model, further research is needed to establish its precise role and underlying mechanisms. Our team is exploring causal gut microbiome-brain mechanisms in ongoing studies. However, further research is necessary to clarify these complex interactions fully. In future genetic studies, we also intend to include additional microglial functional targets and increase the sample size to capture a broader range of responses. Overall, while our study provides valuable insights into the impact of an obesogenic environment on adolescent rats, these limitations underscore the need for further research to comprehend the intricate mechanisms involved in the altered stress responses mediated by dietary obesity.

Data availability statement

The data that support the findings of this study are available from the corresponding author upon reasonable request. Data will be shared following appropriate data use agreements and in accordance with institutional and ethical guidelines.

Funding statement

This work was supported by the National Institutes of Health under grants DK124727, GM060507, and MD006988 and the Loma Linda University School of Medicine GRASP Seed Funds awarded to JDF. The funding entities had no role in the data collection, analysis, interpretation, or manuscript writing.

Ethics approval statement

This study was conducted in accordance with the ethical standards of the Institutional Animal Care and Use Committee (IACUC) under protocol number 20–171 (23–0126), approved by the Loma Linda University Health School of Medicine. This protocol adheres to institutional regulations in accordance with the National Institutes of Health Guide for the Care and Use of Laboratory Animals and follows the ARRIVE guidelines for reporting animal research.

Images and figures

Illustrations were prepared using BioRender (www.biorender.com), OmniGraffle Pro (The Omni Group; Seattle, WA), and GraphPad Prism version 10 (GraphPad Software, San Diego, California USA, www.graphpad.com).

CRediT authorship contribution statement

Perla Ontiveros-Ángel: Conceptualization, Data curation, Formal analysis, Investigation, Methodology, Project administration, Writing – original draft, Writing – review & editing. **Julio David Vega-Torres:** Conceptualization, Formal analysis, Investigation, Methodology, Validation. **Timothy B. Simon:** Formal analysis, Validation, Writing – original draft. **Vivianna Williams:** Investigation, Methodology. **Yaritza Inostroza-Nives:** Conceptualization, Data curation, Investigation, Methodology, Validation, Visualization. **Nashareth Alvarado-Crespo:**

Investigation, Methodology. **Yarimar Vega Gonzalez:** Investigation, Methodology. **Marjory Pompolius:** Formal analysis, Investigation, Methodology. **William Katzka:** Investigation. **John Lou:** Investigation. **Fransua Sharafeddin:** Investigation, Methodology. **Ike De la Peña:** Investigation, Methodology, Resources. **Tien Dong:** Data curation, Formal analysis, Investigation, Methodology, Resources, Validation, Visualization. **Arpana Gupta:** Data curation, Formal analysis, Investigation, Methodology, Resources, Validation, Visualization. **Chi T. Viet:** Data curation, Investigation, Methodology, Visualization. **Marcelo Febo:** Data curation, Formal analysis, Investigation, Methodology, Software, Validation, Visualization. **Andre Obenaus:** Data curation, Investigation, Methodology, Validation, Visualization. **Aarti Nair:** Methodology, Visualization. **Johnny D. Figueroa:** Conceptualization, Formal analysis, Funding acquisition, Investigation, Project administration, Resources, Supervision, Writing – review & editing.

Declaration of generative AI and AI-assisted technologies in the writing process

During the preparation of this work the authors used ChatGPT to improve grammar and readability. After using this tool/service, the authors reviewed and edited the content as needed and take full responsibility for the content of the publication.

Declaration of competing interest

The authors declare no conflicts of interest related to this work.

Data availability

Data will be made available on request.

Acknowledgments

Partial funding for this study was provided by the NIH (DK124727, GM060507, MD006988) and the Loma Linda University School of Medicine GRASP Seed Funds awarded to JDF. The authors thank the Advanced Magnetic Resonance Imaging and Spectroscopy (AMRIS) facility and the National High Magnetic Field Laboratory (NHMFL) for their continued support (National Science Foundation Cooperative Agreement No. DMR-1157490 and the State of Florida). The authors thank the Loma Linda University Animal Care Facility and the cat owners who generously allowed their pets to participate in this study. Furthermore, we would like to extend a special acknowledgment to the cats utilized in this study: Nahla (female) and Chaos (male). Their participation was instrumental in validating the stress model and yielding valuable insights for this study.

Appendix A. Supplementary data

Supplementary data to this article can be found online at https://doi.org/10.1016/j.bbih.2024.100879.

References

Abawi, O., Welling, M.S., Eynde, E., Rossum, E.F.C., Halberstadt, J., Akker, E.L.T., et al., 2020. COVID-19 related anxiety in children and adolescents with severe obesity: a mixed-methods study. Clin Obes 10, e12412.

Adamec, R.E., Shallow, T., 1993. Lasting effects on rodent anxiety of a single exposure to a cat. Physiol. Behav. 54, 101–109.

Adamec, R., Strasser, K., Blundell, J., Burton, P., McKay, D.W., 2006. Protein synthesis and the mechanisms of lasting change in anxiety induced by severe stress. Behav. Brain Res. 167, 270–286.

Asch, R.H., Holmes, S.E., Jastreboff, A.M., Potenza, M.N., Baldassarri, S.R., Carson, R.E., et al., 2021. Lower synaptic density is associated with psychiatric and cognitive alterations in obesity. Neuropsychopharmacology 1–10.

Bakoyiannis, I., Ducourneau, E.G., N'diaye, M., Fermigier, A., Ducroix-Crepy, C., Bosch-Bouju, C., et al., 2024. Obesogenic diet induces circuit-specific memory deficits in mice. Elife 13, e80388.

Balsevich, G., Uribe, A., Wagner, K.V., Hartmann, J., Santarelli, S., Labermaier, C., et al., 2014. Interplay between diet-induced obesity and chronic stress in mice: potential role of FKBP51. J. Endocrinol. 222, 15–26.

Bang, J.Y., Zhao, J., Rahman, M., St-Cyr, S., McGowan, P.O., Kim, J.C., 2022. Hippocampus-anterior hypothalamic circuit modulates stress-induced endocrine and behavioral response. Front. Neural Circ. 16, 894722.

Binder, E.B., Salyakina, D., Lichtner, P., Wochnik, G.M., Ising, M., Pütz, B., et al., 2004. Polymorphisms in FKBP5 are associated with increased recurrence of depressive episodes and rapid response to antidepressant treatment. Nat. Genet. 36, 1319–1325.

Binder, E.B., Bradley, R.G., Liu, W., Epstein, M.P., Deveau, T.C., Mercer, K.B., et al., 2008. Association of FKBP5 polymorphisms and childhood abuse with risk of posttraumatic stress disorder symptoms in adults. JAMA 299, 1291–1305.

Bornstein, S.R., Schuppenies, A., Wong, M.-L., Licinio, J., 2006. Approaching the shared biology of obesity and depression: the stress axis as the locus of gene–environment interactions. Mol. Psychiatr. 11, 892–902.

Bremner, J.D., Moazzami, K., Wittbrodt, M.T., Nye, J.A., Lima, B.B., Gillespie, C.F., et al., 2020. Diet, stress and mental health. Nutrients 12, 2428.

Butler, M.J., Cole, R.M., Deems, N.P., Belury, M.A., Barrientos, R.M., 2020. Fatty food, fatty acids, and microglial priming in the adult and aged hippocampus and amygdala. Brain Behav. Immun. 89, 145–158.

Caetano-Silva, M.E., Rund, L., Hutchinson, N.T., Woods, J.A., Steelman, A.J., Johnson, R. W., 2023. Inhibition of inflammatory microglia by dietary fiber and short-chain fatty acids. Sci Rep-uk 13, 2819.

Calcia, M.A., Bonsall, D.R., Bloomfield, P.S., Selvaraj, S., Barichello, T., Howes, O.D., 2016. Stress and neuroinflammation: a systematic review of the effects of stress on microglia and the implications for mental illness. Psychopharmacology 233, 1–14.

Caslini, M., Bartoli, F., Crocamo, C., Dakanalis, A., Clerici, M., Carrà, G., 2016. Disentangling the association between child abuse and eating disorders. Psychosom. Med. 78, 79–90.

Caso, J.R., MacDowell, K.S., González-Pinto, A., García, S., Diego-Adeliño, J de, Carceller-Sindreu, M., et al., 2021. Gut microbiota, innate immune pathways, and inflammatory control mechanisms in patients with major depressive disorder. Transl. Psychiatry 11, 645.

Cherbuin, N., Sargent-Cox, K., Fraser, M., Sachdev, P., Anstey, K.J., 2015. Being overweight is associated with hippocampal atrophy: the PATH through Life Study. Int. J. Obes. 39, 1509–1514.

Cope, E.C., LaMarca, E.A., Monari, P.K., Olson, L.B., Martinez, S., Zych, A.D., et al., 2018. Microglia play an active role in obesity-associated cognitive decline. J Neurosci Official J Soc Neurosci 38, 8889–8904.

Córdova-Palomera, A., de Reus, M.A., Fatjó-Vilas, M., Falcón, C., Bargalló, N., van den Heuvel, M.P., et al., 2017. FKBP5 modulates the hippocampal connectivity deficits in depression: a study in twins. Brain Imaging Behav 11, 62–75.

Criado-Marrero, M., Smith, T.M., Gould, L.A., Kim, S., Penny, H.J., Sun, Z., et al., 2020. FKBP5 and early life stress affect the hippocampus by an age-dependent mechanism. Brain Behav Immun - Heal 9, 100143.

Cryan, J.F., Dinan, T.G., 2015. Microbiota and neuroimmune signalling—metchnikoff to microglia. Nat Rev Gastroentero 12, 494–496.

Danese, A., Tan, M., 2014. Childhood maltreatment and obesity: systematic review and meta-analysis. Mol. Psychiatr. 19, 544–554.

Davidson, T.L., Kanoski, S.E., Schier, L.A., Clegg, D.J., Benoit, S.C., 2007. A potential role for the hippocampus in energy intake and body weight regulation. Curr. Opin. Pharmacol. 7, 613–616.

Drew, P.D., Chavis, J.A., 2000. Inhibition of microglial cell activation by cortisol. Brain Res. Bull. 52, 391–396.

Erlejman, A.G., Leo, S.A.D., Mazaira, G.I., Molinari, A.M., Camisay, M.F., Fontana, V., et al., 2014. NF-κB transcriptional activity is modulated by FK506-binding proteins FKBP51 and FKBP52. J. Biol. Chem. 289, 26263–26276.

Erny, D., Prinz, M., 2020. How microbiota shape microglial phenotypes and epigenetics. Glia 68, 1655–1672.

Erny, D., Angelis, ALH de, Jaitin, D., Wieghofer, P., Staszewski, O., David, E., et al., 2015. Host microbiota constantly control maturation and function of microglia in the CNS. Nat. Neurosci. 18, 965–977.

Fani, N., Gutman, D., Tone, E.B., Almli, L., Mercer, K.B., Davis, J., et al., 2013. FKBP5 and attention bias for threat: associations with hippocampal function and shape. Jama Psychiat 70, 392–400.

Felger, J.C., 2018. Imaging the role of inflammation in mood and anxiety-related disorders. Curr. Neuropharmacol. 16, 533–558.

Francella, C., Green, M., Caspani, G., Lai, J.K.Y., Rilett, K.C., Foster, J.A., 2022. Microbe–immune–stress interactions impact behaviour during postnatal development. Int. J. Mol. Sci. 23, 15064.

Frank, M.G., Fonken, L.K., Watkins, L.R., Maier, S.F., 2019. Microglia: neuroimmune-sensors of stress. Semin. Cell Dev. Biol. 94, 176–185.

Gan, Y.-L., Wang, C.-Y., He, R.-H., Hsu, P.-C., Yeh, H.-H., Hsieh, T.-H., et al., 2022. FKBP51 mediates resilience to inflammation-induced anxiety through regulation of glutamic acid decarboxylase 65 expression in mouse hippocampus. J Neuroinflamm 19, 152.

Grillon, C., Baas, J., 2003. A review of the modulation of the startle reflex by affective states and its application in psychiatry. Clin. Neurophysiol. 114, 1557–1579.

Guedes, J.R., Ferreira, P.A., Costa, J.M., Cardoso, A.L., Peça, J., 2022. Microglia-dependent remodeling of neuronal circuits. J. Neurochem. 163, 74–93.

Guillemot-Legris, O., Muccioli, G.G., 2017. Obesity-induced neuroinflammation: beyond the hypothalamus. Trends Neurosci. 40, 237–253.

Hao, S., Dey, A., Yu, X., Stranahan, A.M., 2016. Dietary obesity reversibly induces synaptic stripping by microglia and impairs hippocampal plasticity. Brain Behav. Immun. 51, 230–239.

Haroon, E., Daguanno, A.W., Woolwine, B.J., Goldsmith, D.R., Baer, W.M., Wommack, E. C., et al., 2018. Antidepressant treatment resistance is associated with increased inflammatory markers in patients with major depressive disorder. Psychoneuroendocrinology 95, 43–49.
Häusl, A.S., Balsevich, G., Gassen, N.C., Schmidt, M.V., 2019. Focus on FKBP51: a molecular link between stress and metabolic disorders. Mol. Metabol. 29, 170–181.
He, H., He, H., Mo, L., You, Z., Zhang, J., 2024. Priming of microglia with dysfunctional gut microbiota impairs hippocampal neurogenesis and fosters stress vulnerability of mice. Brain Behav. Immun. 115, 280–294.
Herman, J.P., Patel, P.D., Akil, H., Watson, S.J., 1989. Localization and regulation of glucocorticoid and mineralocorticoid receptor messenger RNAs in the hippocampal formation of the rat. Mol. Endocrinol. 3, 1886–1894.
Herman, J.P., Dolgas, C.M., Carlson, S.L., 1998. Ventral subiculum regulates hypothalamo–pituitary–adrenocortical and behavioural responses to cognitive stressors. Neuroscience 86, 449–459.
Huang, Y., Wu, J., Zhang, H., Li, Y., Wen, L., Tan, X., et al., 2023. The gut microbiome modulates the transformation of microglial subtypes. Mol. Psychiatr. 28, 1611–1621.
Imperatori, C., Innamorati, M., Lamis, D.A., Farina, B., Pompili, M., Contardi, A., et al., 2016. Childhood trauma in obese and overweight women with food addiction and clinical-level of binge eating. Child Abuse Neglect 58, 180–190.
Jacka, F.N., Cherbuin, N., Anstey, K.J., Sachdev, P., Butterworth, P., 2015. Western diet is associated with a smaller hippocampus: a longitudinal investigation. BMC Med. 13 (1), 9.
Jacobson, L., Sapolsky, R., 1991. The role of the hippocampus in feedback regulation of the hypothalamic-pituitary-adrenocortical axis. Endocr. Rev. 12, 118–134.
Jiang, H., Ling, Z., Zhang, Y., Mao, H., Ma, Z., Yin, Y., et al., 2015. Altered fecal microbiota composition in patients with major depressive disorder. Brain Behav. Immun. 48, 186–194.
Jimenez, J.C., Su, K., Goldberg, A.R., Luna, V.M., Biane, J.S., Ordek, G., et al., 2018. Anxiety cells in a hippocampal-hypothalamic circuit. Neuron 97, 670–683.e6.
Johnson, F.K., Kaffman, A., 2018. Early life stress perturbs the function of microglia in the developing rodent brain: new insights and future challenges. Brain Behav. Immun. 69, 18–27.
Johnson, J.D., Barnard, D.F., Kulp, A.C., Mehta, D.M., 2019. Neuroendocrine regulation of brain cytokines after psychological stress. J Endocr Soc 3, 1302–1320.
Kalyan-Masih, P., Vega-Torres, J.D., Miles, C., Haddad, E., Rainsbury, S., Baghchechi, M., et al., 2016. Western High-Fat Diet Consumption during Adolescence Increases Susceptibility to Traumatic Stress while Selectively Disrupting Hippocampal and Ventricular Volumes, 3. Eneuro 2016, p. 16. ENEURO.0125.
Karperien, A.L., Jelinek, H.F., 2015. Fractal, multifractal, and lacunarity analysis of microglia in tissue engineering. Front. Bioeng. Biotechnol. 3, 51.
Kästle, M., Kistler, B., Lamla, T., Bretschneider, T., Lamb, D., Nicklin, P., et al., 2018. FKBP51 modulates steroid sensitivity and NFκB signalling: a novel anti-inflammatory drug target. Eur. J. Immunol. 48, 1904–1914.
Kemp, G.M., Altimimi, H.F., Nho, Y., Heir, R., Klyczek, A., Stellwagen, D., 2022. Sustained TNF signaling is required for the synaptic and anxiety-like behavioral response to acute stress. Mol. Psychiatr. 27, 4474–4484.
Koch, M., Schnitzler, H.-U., 1997. The acoustic startle response in rats—circuits mediating evocation, inhibition and potentiation. Behav. Brain Res. 89, 35–49.
Kohl, S.H., Veit, R., Spetter, M.S., Günther, A., Rina, A., Lührs, M., et al., 2019. Real-time fMRI neurofeedback training to improve eating behavior by self-regulation of the dorsolateral prefrontal cortex: a randomized controlled trial in overweight and obese subjects. Neuroimage 191, 596–609.
Kosugi, K., Yoshida, K., Suzuki, T., Kobayashi, K., Yoshida, K., Mimura, M., et al., 2021. Activation of ventral CA1 hippocampal neurons projecting to the lateral septum during feeding. Hippocampus 31, 294–304.
Kreisel, T., Frank, M.G., Licht, T., Reshef, R., Ben-Menachem-Zidon, O., Baratta, M.V., et al., 2014. Dynamic microglial alterations underlie stress-induced depressive-like behavior and suppressed neurogenesis. Mol. Psychiatr. 19, 699–709.
Land, B.B., Narayanan, N.S., Liu, R.-J., Gianessi, C.A., Brayton, C.E., Grimaldi, D.M., et al., 2014. Medial prefrontal D1 dopamine neurons control food intake. Nat. Neurosci. 17, 248–253.
Lange, S.J., Kompaniyets, L., Freedman, D.S., Kraus, E.M., Porter DNP3, R., et al., 2021. Longitudinal trends in body mass index before and during the COVID-19 pandemic among persons aged 2–19 Years — United States, 2018–2020. Morbidity Mortal Wkly Rep 70, 1278–1283.
Li, S., Liao, Y., Dong, Y., Li, X., Li, J., Cheng, Y., et al., 2021. Microglial deletion and inhibition alleviate behavior of post-traumatic stress disorder in mice. J Neuroinflamm 18, 7.
Locke, A.E., Kahali, B., Berndt, S.I., Justice, A.E., Pers, T.H., Day, F.R., et al., 2015. Genetic studies of body mass index yield new insights for obesity biology. Nature 518, 197–206.
Lopresti, A.L., Drummond, P.D., 2013. Obesity and psychiatric disorders: commonalities in dysregulated biological pathways and their implications for treatment. Prog Neuro-psychopharmacology Biological Psychiatry 45, 92–99.
Lowe, C.J., Reichelt, A.C., Hall, P.A., 2019. The prefrontal cortex and obesity: a health neuroscience perspective. Trends Cognit. Sci. 23, 349–361.
Lu, Z., Liu, S., Lopes-Virella, M.F., Wang, Z., 2021. LPS and palmitic acid Co-upregulate microglia activation and neuroinflammatory response. Compr Psychoneuroendocrinology 6, 100048.
Lynch, C.M.K., Clarke, G., Cryan, J.F., 2021. Powering up microbiome-microglia interactions. Cell Metabol. 33, 2097–2099.
Margolis, K.G., Cryan, J.F., Mayer, E.A., 2021. The microbiota-gut-brain Axis: from motility to mood. Gastroenterology 160, 1486–1501.
Masodkar, K., Johnson, J., Peterson, M.J., 2016. A review of posttraumatic stress disorder and obesity: exploring the link. Prim Care Companion Cns Disord 18. https://doi.org/10.4088/pcc.15r01848.
Mayer, E.A., Tillisch, K., Gupta, A., 2015. Gut/brain axis and the microbiota. J. Clin. Invest. 125, 926–938.
McEwen, B.S., 2001. Plasticity of the Hippocampus: adaptation to chronic stress and allostatic load. Ann Ny Acad Sci 933, 265–277.
McLaughlin, K.A., Koenen, K.C., Hill, E.D., Petukhova, M., Sampson, N.A., Zaslavsky, A. M., et al., 2013. Trauma exposure and posttraumatic stress disorder in a national sample of adolescents. J. Am. Acad. Child Adolesc. Psychiatry 52, 815–830.e14.
Medina, A.M., Mejia, V.Y., Schell, A.M., Dawson, M.E., Margolin, G., 2001. Startle reactivity and PTSD symptoms in a community sample of women. Psychiatr. Res. 101, 157–169.
Mestre, Z.L., Bischoff-Grethe, A., Eichen, D.M., Wierenga, C.E., Strong, D., Boutelle, K.N., 2017. Hippocampal atrophy and altered brain responses to pleasant tastes among obese compared with healthy weight children. Int. J. Obes. 41, 1496–1502.
Michels, N., Wiele, TV de, Fouhy, F., O'Mahony, S., Clarke, G., Keane, J., 2019. Gut microbiome patterns depending on children's psychosocial stress: reports versus biomarkers. Brain Behav. Immun. 80, 751–762.
Michopoulos, V., Vester, A., Neigh, G., 2016. Posttraumatic stress disorder: a metabolic disorder in disguise? Exp. Neurol. 284, 220–229.
Milaneschi, Y., Simmons, W.K., van Rossum, E.F.C., Penninx, B.W., 2019. Depression and obesity: evidence of shared biological mechanisms. Mol. Psychiatr. 24, 18–33.
Moreno, L.A., Rodriguez, G., Fleta, J., Bueno-Lozano, M., Lazaro, A., Bueno, G., 2010. Trends of dietary habits in adolescents. Crit Rev Food Sci 50, 106–112.
Mosher, K.I., Wyss-Coray, T., 2015. Go with your gut: microbiota meet microglia. Nat. Neurosci. 18, 930–931.
Natividad, J.M., Lamas, B., Pham, H.P., Michel, M.-L., Rainteau, D., Bridonneau, C., et al., 2018. Bilophila wadsworthia aggravates high fat diet induced metabolic dysfunctions in mice. Nat. Commun. 9, 2802.
Nelson, L.H., Peketi, P., Lenz, K.M., 2021. Microglia regulate cell genesis in a sex-dependent manner in the neonatal Hippocampus. Neuroscience 453, 237–255.
Nikolova, V.L., Hall, M.R.B., Hall, L.J., Cleare, A.J., Stone, J.M., Young, A.H., 2021. Perturbations in gut microbiota composition in psychiatric disorders. JAMA Psychiatr. 78, 1343–1354.
Ohgidani, M., Kato, T.A., Sagata, N., Hayakawa, K., Shimokawa, N., Sato-Kasai, M., et al., 2016. TNF-α from hippocampal microglia induces working memory deficits by acute stress in mice. Brain Behav. Immun. 55, 17–24.
Opel, N., Thalamuthu, A., Milaneschi, Y., Grotegerd, D., Flint, C., Leenings, R., et al., 2020. Brain structural abnormalities in obesity: relation to age, genetic risk, and common psychiatric disorders. Mol. Psychiatr. 1–14.
Organization WH, 2016. Report of the Commission on Ending Childhood Obesity. World Health Organization, Geneva. https://apps.who.int/iris/handle/10665/204176.
Ornitz, E.M., Pynoos, R.S., 1989. Startle modulation in children with posttraumatic stress disorder. Am. J. Psychiatr. 146, 866–870.
Osimo, E.F., Pillinger, T., Rodriguez, I.M., Khandaker, G.M., Pariante, C.M., Howes, O.D., 2020. Inflammatory markers in depression: a meta-analysis of mean differences and variability in 5,166 patients and 5,083 controls. Brain Behav. Immun. 87, 901–909.
Paolicelli, R.C., Bolasco, G., Pagani, F., Maggi, L., Scianni, M., Panzanelli, P., et al., 2011. Synaptic pruning by microglia is necessary for normal brain development. Science 333, 1456–1458.
Pérez-Reytor, D., Puebla, C., Karahanian, E., García, K., 2021. Use of short-chain fatty acids for the recovery of the intestinal epithelial barrier affected by bacterial toxins. Front. Physiol. 12, 650313.
Perkonigg, A., Owashi, T., Stein, M.B., Kirschbaum, C., Wittchen, H.-U., 2009. Posttraumatic stress disorder and obesity evidence for a risk association. Am. J. Prev. Med. 36, 1–8.
Picard, K., Bisht, K., Poggini, S., Garofalo, S., Golia, M.T., Basilico, B., et al., 2021. Microglial-glucocorticoid receptor depletion alters the response of hippocampal microglia and neurons in a chronic unpredictable mild stress paradigm in female mice. Brain Behav. Immun. 97, 423–439.
Pohl, J., Sheppard, M., Luheshi, G.N., Woodside, B., 2014. Diet-induced weight gain produces a graded increase in behavioral responses to an acute immune challenge. Brain Behav. Immun. 35, 43–50.
Raji, C.A., Ho, A.J., Parikshak, N.N., Becker, J.T., Lopez, O.L., Kuller, L.H., et al., 2010. Brain structure and obesity. Hum. Brain Mapp. 31, 353–364.
Rea, K., Dinan, T.G., Cryan, J.F., 2016. The microbiome: a key regulator of stress and neuroinflammation. Neurobiology Stress 4, 23–33.
Reemst, K., Kracht, L., Kotah, J.M., Rahimian, R., van Irsen, A.A.S., Sotomayor, G.C., et al., 2022. Early-life stress lastingly impacts microglial transcriptome and function under basal and immune-challenged conditions. Transl. Psychiatry 12, 507.
Reyes, R.E.N., Zhang, Z., Gao, L., Asatryan, L., 2020. Microbiome meets microglia in neuroinflammation and neurological disorders. Neuroimmunol. Neuroinflammation 2020. https://doi.org/10.20517/2347-8659.2020.13.
Russo, C.D., Cappoli, N., Coletta, I., Mezzogori, D., Paciello, F., Pozzoli, G., et al., 2018. The human microglial HMC3 cell line: where do we stand? A systematic literature review. J Neuroinflamm 15, 259.
Salari-Moghaddam, A., Keshteli, A.H., Afshar, H., Esmaillzadeh, A., Adibi, P., 2018. Association between dietary inflammatory index and psychological profile in adults. Clin. Nutr. https://doi.org/10.1016/j.clnu.2018.10.015.
Santana, J.M.S., Vega-Torres, J.D., Ontiveros-Angel, P., Lee, J.B., Torres, Y.A., Gonzalez, A.Y.C., et al., 2021. Oxidative stress and neuroinflammation in a rat model of co-morbid obesity and psychogenic stress. Behav. Brain Res. 400, 112995.
Sapolsky, R.M., Krey, L.C., McEwen, B.S., 1984. Glucocorticoid-sensitive hippocampal neurons are involved in terminating the adrenocortical stress response. Proc. Natl. Acad. Sci. U.S.A. 81, 6174–6177.

Schafer, D.P., Stevens, B., 2013. Phagocytic glial cells: sculpting synaptic circuits in the developing nervous system. Curr. Opin. Neurobiol. 23, 1034–1040.
Schmidt, U., Buell, D.R., Ionescu, I.A., Gassen, N.C., Holsboer, F., Cox, M.B., et al., 2015. A role for synapsin in FKBP51 modulation of stress responsiveness: convergent evidence from animal and human studies. Psychoneuroendocrino 52, 43–58.
Schoenfeld, T.J., Rhee, D., Martin, L., Smith, J.A., Sonti, A.N., Padmanaban, V., et al., 2019. New neurons restore structural and behavioral abnormalities in a rat model of PTSD. Hippocampus 29, 848–861.
Scott, K.M., McGee, M.A., Wells, J.E., Browne, M.A.O., 2008. Obesity and mental disorders in the adult general population. J. Psychosom. Res. 64, 97–105.
Sert, NP du, Hurst, V., Ahluwalia, A., Alam, S., Avey, M.T., Baker, M., et al., 2020. The ARRIVE guidelines 2.0: updated guidelines for reporting animal research. PLoS Biol. 18, e3000410.
Sharafeddin, F., Sierra, J., Ghaly, M., Simon, T.B., Ontiveros-Ángel, P., Edelbach, B, Febo, M, Labus, J, Figueroa, J.D., 2024. Role of the prefrontal cortical protease TACE/ADAM17 in neurobehavioral responses to chronic stress during adolescence. Brain Behav 14 (5), e3482.
Simon, G.E., Korff, M.V., Saunders, K., Miglioretti, D.L., Crane, P.K., Belle, G van, et al., 2006. Association between obesity and psychiatric disorders in the US adult population. Arch. Gen. Psychiatr. 63, 824–830.
Sobesky, J.L., Barrientos, R.M., May, H.S.D., Thompson, B.M., Weber, M.D., Watkins, L. R., et al., 2014. High-fat diet consumption disrupts memory and primes elevations in hippocampal IL-1β, an effect that can be prevented with dietary reversal or IL-1 receptor antagonism. Brain Behav. Immun. 42, 22–32.
Socała, K., Doboszewska, U., Szopa, A., Serefko, A., Włodarczyk, M., Zielińska, A., et al., 2021. The role of microbiota-gut-brain axis in neuropsychiatric and neurological disorders. Pharmacol. Res. 172, 105840.
Tozzi, L., Farrell, C., Booij, L., Doolin, K., Nemoda, Z., Szyf, M., et al., 2018. Epigenetic changes of FKBP5 as a link connecting genetic and environmental risk factors with structural and functional brain changes in major depression. Neuropsychopharmacology 43, 1138–1145.
Tracy, L.M., Bergqvist, F., Ivanova, E.V., Jacobsen, K.T., Iverfeldt, K., 2013. Exposure to the saturated free fatty acid palmitate alters BV-2 microglia inflammatory response. J. Mol. Neurosci. 51, 805–812.
Trivedi, M.A., Coover, G.D., 2006. Neurotoxic lesions of the dorsal and ventral hippocampus impair acquisition and expression of trace-conditioned fear-potentiated startle in rats. Behav. Brain Res. 168, 289–298.
Ulrich-Lai, Y.M., Herman, J.P., 2009. Neural regulation of endocrine and autonomic stress responses. Nat. Rev. Neurosci. 10, 397–409.
Ulrich-Lai, Y.M., Fulton, S., Wilson, M., Petrovich, G., Rinaman, L., 2015. Stress exposure, food intake and emotional state. Ann Ny Acad Sci 18, 381–399.
Vega-Torres, J.D., Haddad, E., Lee, J.B., Kalyan-Masih, P., George, W.I.M., Pérez, L.L., et al., 2018. Exposure to an obesogenic diet during adolescence leads to abnormal maturation of neural and behavioral substrates underpinning fear and anxiety. Brain Behav. Immun. 70, 96–117. https://doi.org/10.1016/j.bbi.2018.01.011.
Vega-Torres, J.D., Kalyan-Masih, P., Argueta, D.A., DiPatrizio, N.V., Figueroa, J.D., 2019. Endocrine, metabolic, and endocannabinoid alterations in rats exhibiting high anxiety-related behaviors. bioRxiv, 605329.
Vega-Torres, J.D., Azadian, M., Rios-Orsini, R.A., Reyes-Rivera, A.L., Ontiveros-Angel, P., Figueroa, J.D., 2020. Adolescent vulnerability to heightened emotional reactivity and anxiety after brief exposure to an obesogenic diet. Front Neurosci-switz 14, 562.
Vega-Torres, J.D., Ontiveros-Angel, P., Terrones, E., Stuffle, E.C., Solak, S., Tyner, E., et al., 2022a. Short-term exposure to an obesogenic diet during adolescence elicits anxiety-related behavior and neuroinflammation: modulatory effects of exogenous neuregulin-1. Transl. Psychiatry 12, 83.
Vega-Torres, J.D., Ontiveros-Angel, P., Terrones, E., Stuffle, E.C., Solak, S., Tyner, E., et al., 2022b. Short-term exposure to an obesogenic diet during adolescence elicits anxiety-related behavior and neuroinflammation: modulatory effects of exogenous neuregulin-1. Transl. Psychiatry 12, 83.
Vidal, J., Bie, J de, Granneman, R.A., Wallinga, A.E., Koolhaas, J.M., Buwalda, B., 2007. Social stress during adolescence in Wistar rats induces social anxiety in adulthood without affecting brain monoaminergic content and activity. Physiol. Behav. 92, 824–830.
Wagner, K.V., Marinescu, D., Hartmann, J., Wang, X.-D., Labermaier, C., Scharf, S.H., et al., 2012. Differences in FKBP51 regulation following chronic social defeat stress correlate with individual stress sensitivity: influence of paroxetine treatment. Neuropsychopharmacology 37, 2797–2808.
Wang, G.-J., Volkow, N.D., Logan, J., Pappas, N.R., Wong, C.T., Zhu, W., et al., 2001. Brain dopamine and obesity. Lancet 357, 354–357.
Wang, Z., Liu, D., Wang, F., Liu, S., Zhao, S., Ling, E.-A., et al., 2012a. Saturated fatty acids activate microglia via Toll-like receptor 4/NF-κB signalling. Br. J. Nutr. 107, 229–241.
Wang, Z., Liu, D., Wang, F., Liu, S., Zhao, S., Ling, E.-A., et al., 2012b. Saturated fatty acids activate microglia via Toll-like receptor 4/NF-κB signalling. Br. J. Nutr. 107, 229–241.
Willmer, T., Goedecke, J.H., Dias, S., Louw, J., Pheiffer, C., 2020. DNA methylation of FKBP5 in South African women: associations with obesity and insulin resistance. Clin. Epigenet. 12, 141.
Wit, DF de, Hanssen, N.M.J., Wortelboer, K., Herrema, H., Rampanelli, E., Nieuwdorp, M., 2023. Evidence for the contribution of the gut microbiome to obesity and its reversal. Sci. Transl. Med. 15, eadg2773.
Wolf, E.J., Miller, D.R., Logue, M.W., Sumner, J., Stoop, T.B., Leritz, E.C., et al., 2017. Contributions of polygenic risk for obesity to PTSD-related metabolic syndrome and cortical thickness. Brain Behav. Immun. 65, 328–336.
Womersley, J.S., Nothling, J., Toikumo, S., Malan-Müller, S., Heuvel, L.L., McGregor, N. W., et al., 2022. Childhood trauma, the stress response and metabolic syndrome: a focus on DNA methylation. Eur. J. Neurosci. 55, 2253–2296.
Woolford, S.J., Sidell, M., Li, X., Else, V., Young, D.R., Resnicow, K., et al., 2021. Changes in body mass index among children and adolescents during the COVID-19 pandemic. JAMA 326, 1434–1436.
Workman, J.L., Gobinath, A.R., Kitay, N.F., Chow, C., Brummelte, S., Galea, L.A.M., 2016. Parity modifies the effects of fluoxetine and corticosterone on behavior, stress reactivity, and hippocampal neurogenesis. Neuropharmacology 105, 443–453.
Wu, G.D., Chen, J., Hoffmann, C., Bittinger, K., Chen, Y.-Y., Keilbaugh, S.A., et al., 2011. Linking long-term dietary patterns with gut microbial enterotypes. Science 334, 105–108.
Xu, Z., Jiang, W., Huang, W., Lin, Y., Chan, F.K.L., Ng, S.C., 2022. Gut microbiota in patients with obesity and metabolic disorders — a systematic review. Genes Nutrition 17, 2.
Xu, B., Lang, L.-M., Li, S.-Z., Guo, J.-R., Wang, J.-F., Yang, H.-M., et al., 2019. Microglia activated by excess cortisol induce HMGB1 acetylation and neuroinflammation in the hippocampal DG region of mice following cold exposure. Biomol 9, 426.
Yehuda, R., Daskalakis, N.P., Bierer, L.M., Bader, H.N., Klengel, T., Holsboer, F., et al., 2016. Holocaust exposure induced intergenerational effects on FKBP5 methylation. Biol. Psychiatr. 80, 372–380.
Yusupov, N., Doeselaar, L., Röh, S., Wiechmann, T., Ködel, M., Sauer, S., et al., 2023. Extensive evaluation of DNA methylation of functional elements in the murine Fkbp5 locus using high-accuracy DNA methylation measurement via targeted bisulfite sequencing. Eur. J. Neurosci. 58, 2662–2676.
Zobel, A., Schuhmacher, A., Jessen, F., Höfels, S., Widdern, O von, Metten, M., et al., 2010. DNA sequence variants of the FKBP5 gene are associated with unipolar depression. Int. J. Neuropsychopharmacol. 13, 649–660.
Zoladz, P.R., Fleshner, M., Diamond, D.M., 2012. Psychosocial animal model of PTSD produces a long-lasting traumatic memory, an increase in general anxiety and PTSD-like glucocorticoid abnormalities. Psychoneuroendocrinology 37, 1531–1545.
Zoladz, P.R., Park, C.R., Fleshner, M., Diamond, D.M., 2015. Psychosocial predator-based animal model of PTSD produces physiological and behavioral sequelae and a traumatic memory four months following stress onset. Physiol. Behav. 147, 183–192.